CHEMISTRY
A European Journal

Supporting Information

A Coumarin Triflate Reagent Enables One-Step Synthesis of Photo-Caged Lipid Metabolites for Studying Cell Signaling

Nicolai Wagner[+], Milena Schuhmacher[+], Annett Lohmann, and André Nadler*[a]

chem_201903909_sm_miscellaneous_information.pdf

1. Supplementary figures

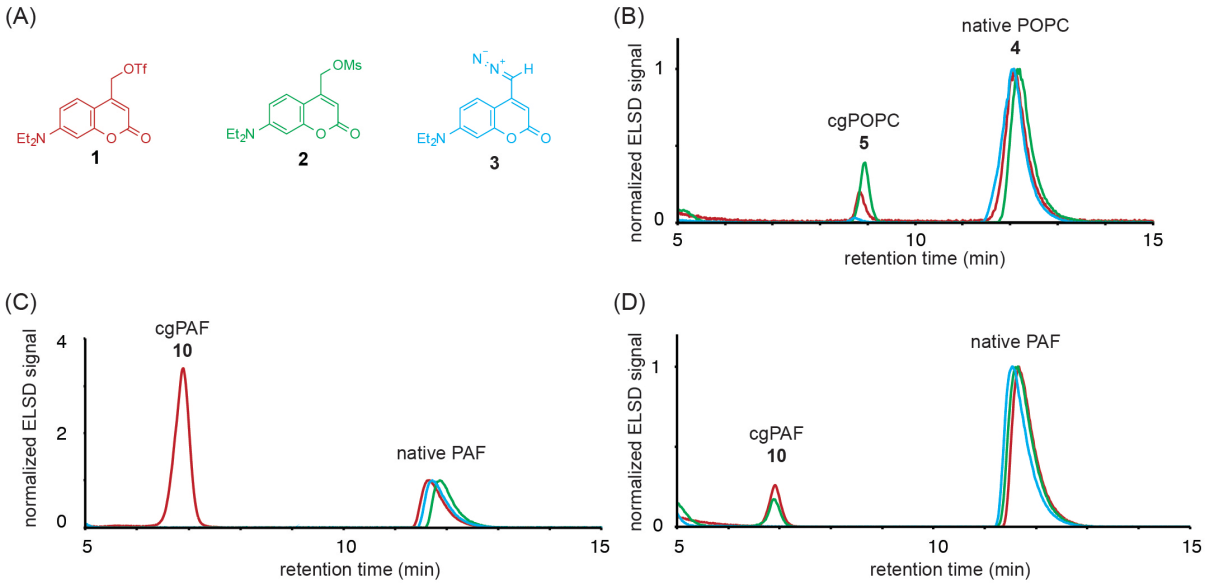

Supplementary Figure S1. HPLC chromatograms displaying the conversion of the phospholipids POPC (4) and PAF into caged POPC (5) and caged PAF using different coumarin reagents. Red traces: Coumarin triflate reagent (**1**), green traces: Coumarin mesylate reagent (**2**), blue traces: Coumarin diazo reagent (**3**). Reaction conditions were kept constant with regard to utilized base, reaction time, temperature and solvent. (A) Structures of utilized coumarin reagents. (B) Chromatograms of POPC conversion, reaction conditions: 60 ºC, DIEA, 20 h, DMSO/acetonitrile/chloroform mixture (Method B). (C) Chromatograms of PAF conversion, reaction conditions: 0 ºC, DIEA, 3 h, DCM and chloroform mixture (Method A) (D) Chromatograms of PAF conversion, reaction conditions: 60 ºC, DIEA, 20 h, DMSO/acetonitrile/chloroform mixture (Method B). Chromatograms were acquired using a light scattering detector (see methods for details) to monitor both POPC/PAF and photo-caged POPC/PAF in the same acquisition mode. Using Method A (C, Figure 1A), conversion was only observed using the coumarin triflate reagent (**1**). Under harsh conditions of Method B (PAF: D; POPC: B), a low amount of conversion was observed using the coumarin triflate reagent (**1**) and the coumarin mesylate (**2**). Data are normalized to the respective POPC/PAF signal. Experimental details can be found in section 8.

(A)

compound	absorption max. (nm)	extinction coefficient ($L*mol^{-1}*cm^{-1}$)	quantum yield
5	380	25835.42	0.03
6	376	27543.09	0.35
7	376	27638.51	0.60
9	380	49702.18	0.34
10	382	30980.11	0.04
11	382	18468.83	0.02
12	382	23420.11	0.02
13	380	43834.90	0.35
14	380	35901.49	0.18
15	380	42236.56	0.13

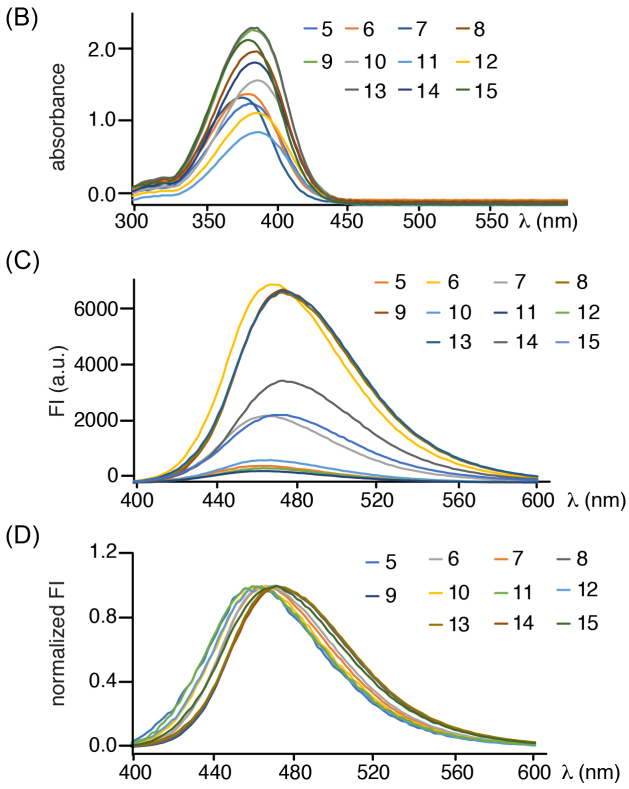

Supplementary Figure S2. Photophysical properties of new caged compounds 5, 7, 10-15. (A) Table listing the absorption maxima, extinction coefficient and quantum yield of the new, photo-caged compounds. For the determination of the quantum yield, caged AA was used as a reference[1]. (B) Absorption spectra of the new, photo-caged compounds at a concentration of 250 µM. (C) Emission spectra of new, photo-caged compounds at a concentration of 31.25 µM (except for **7** with a concentration of 7.8 µM). (D) Normalized emission spectra of new, photo-caged compounds. The relatively large differences in fluorescence quantum yields are likely due to the fact that the coumarin chromophore is decorated with chemically diverse substituents at the hydroxy-methylene group (ester groups, phosphodi- and phosphotriester groups).

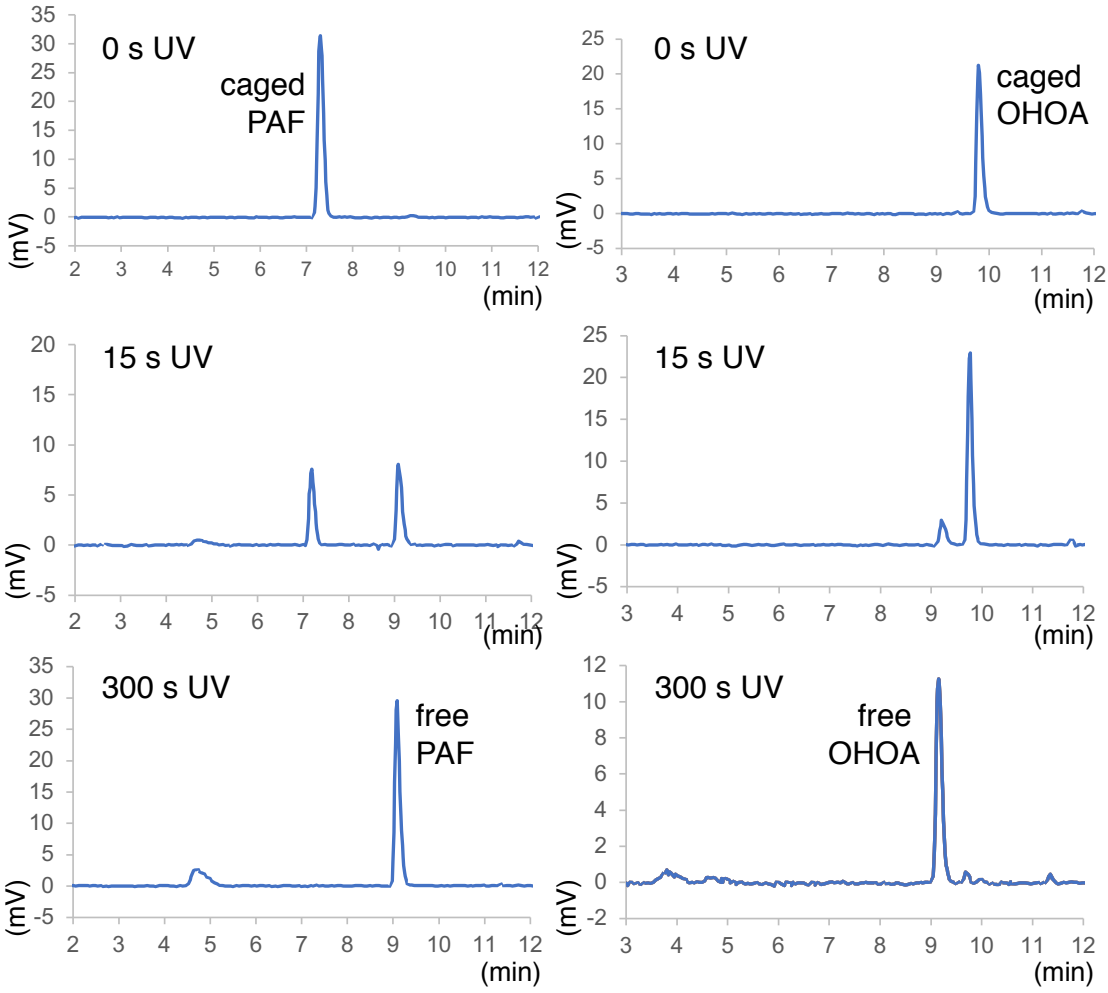

Supplementary Figure S3. Confirmation of photorelease of the parent compounds form new, photo-caged compounds. Exemplary chromatograms are shown of caged PAF (**10**, left) and caged OHOA (**14**, right) after 0 s, 15 s and 300 s of UV illumination using a UV lamp. With longer illumination time, the initial peaks (ELSD signals) disappear and new peaks are forming, which match the retention times of the parent molecules, free PAF and free OHOA. The results for **5**, **7**, **9**-**15** are listed in Supplementary Table 7.

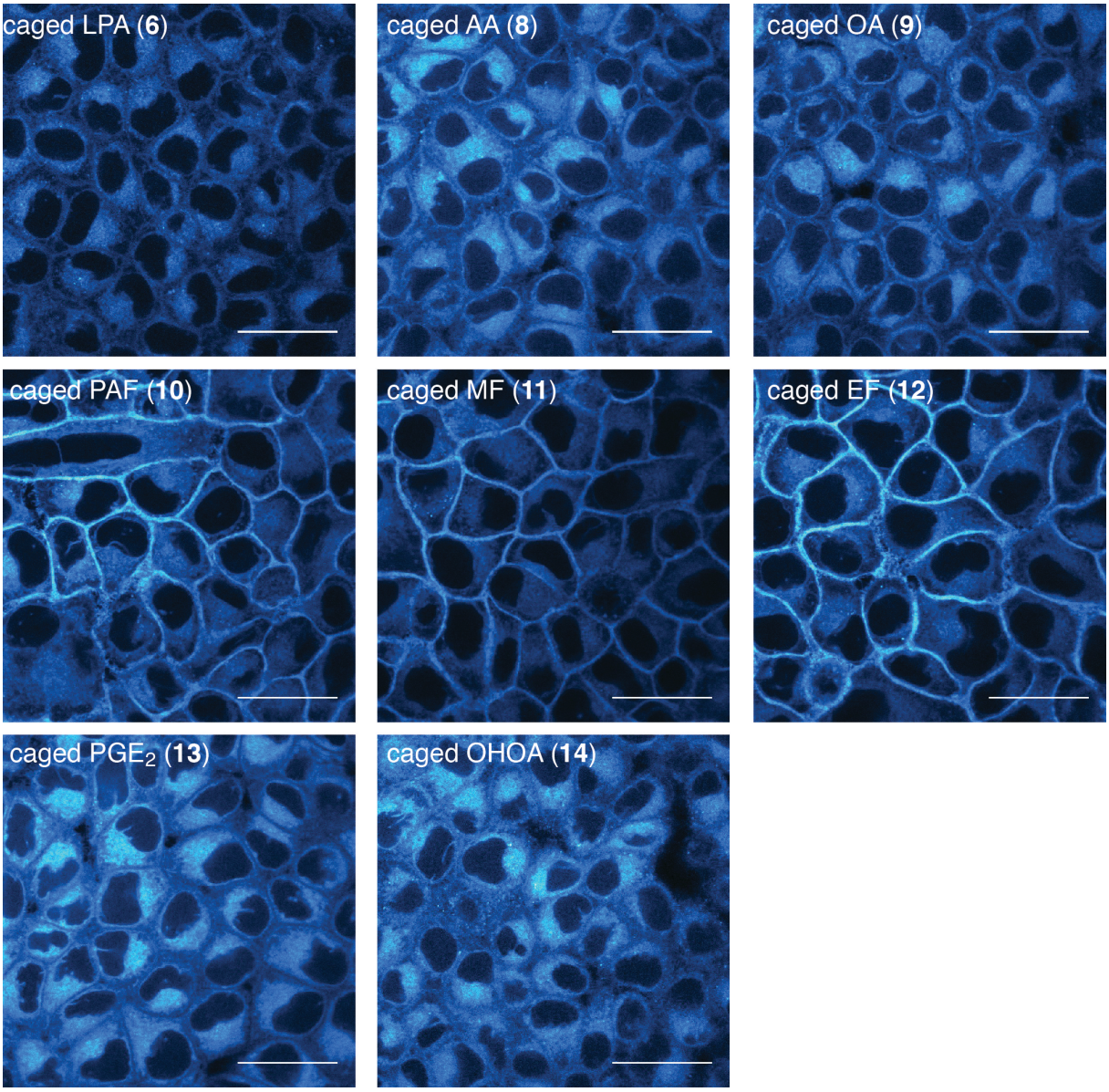

Supplementary Figure S4. Intracellular localization of compounds 6, 8-14. Fluorescence images displaying larger fields of view and higher cell numbers at the same acquisition conditions as used for Fig. 1e. Scale bars indicate 30 µm. Compounds were loaded for 10 min in a 10 µM loading solution.

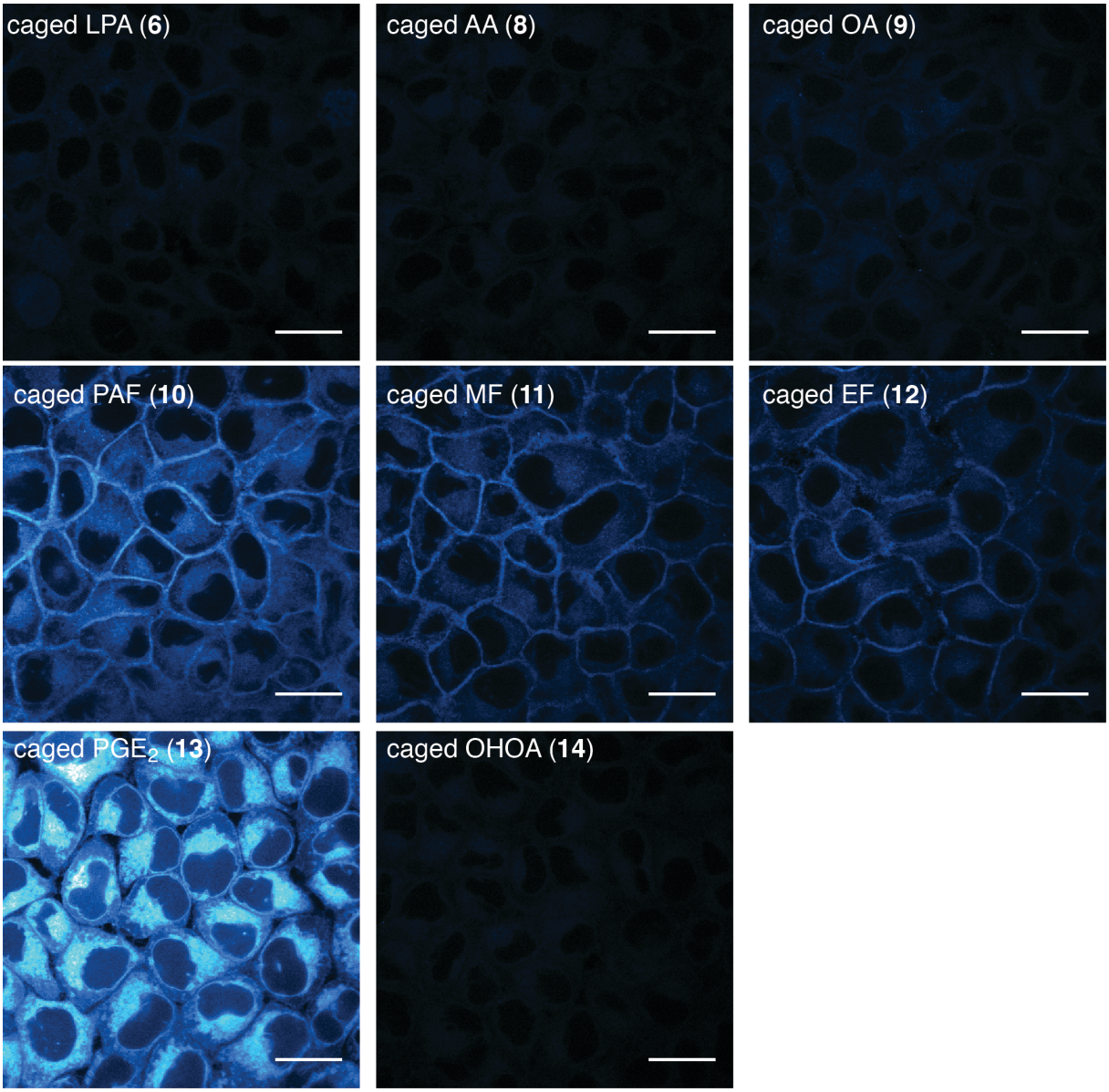

Supplementary Figure S5. Different uptake of compounds 6, 8-14 in Hela Kyoto cells. Fluorescence intensities vary significantly when loading the same amount of compound for all caged molecules. Fluorescence images were acquired using identical acquisition conditions. Scale bars indicate 25 µm. Compounds were loaded for 10 min using a 20 µM loading solution.

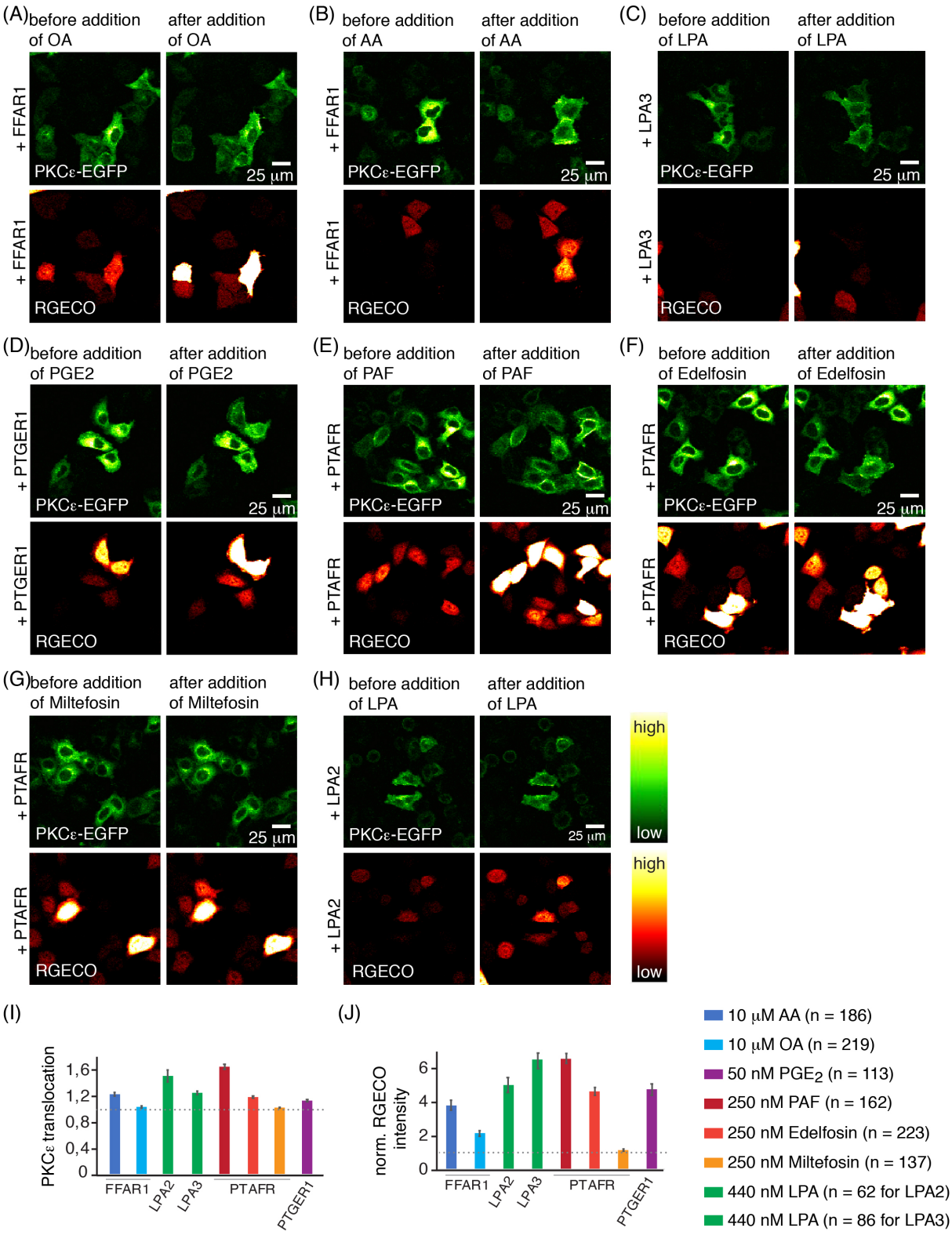

Supplementary Figure S6. Addition of free GPCR ligands to HeLa Kyoto cells expressing the corresponding GPCRs. Robust Ca^{2+} transients and/or PKC recruitment were observed for all conditions except for miltefosin. (A, B) Cellular localization of PKCε-EGFP and RGECO fluorescence intensity before and after addition of arachidonic acid (AA) (A) and oleic acid (OA) (B) to HeLa Kyoto cells overexpressing FFAR1. (C) Cellular localization of PKCε-EGFP and RGECO fluorescence intensity before and after addition of lysophosphatidic acid (LPA) to HeLa Kyoto cells overexpressing of LPA3. (D) Cellular localization of PKCε-EGFP and RGECO fluorescence intensity before and after addition of prostaglandin E_2 (PGE_2) to HeLa Kyoto cells overexpressing PTGER1. (E) Cellular localization of PKCε-EGFP and RGECO fluorescence intensity before and after addition of platelet activating factor (PAF) to HeLa Kyoto cells overexpressing PTAFR. (F) Cellular localization of PKCε-EGFP and RGECO fluorescence intensity before and after addition of edelfosin to HeLa Kyoto cells overexpressing PTAFR. (G) Cellular localization of PKCε-EGFP and RGECO fluorescence intensity before and after addition

of miltefosin to HeLa Kyoto cells overexpressing PTAFR. (H) Cellular localization of PKCε-EGFP and RGECO fluorescence intensity before and after addition of lysophosphatidic acid (LPA) to HeLa Kyoto cells overexpressing of LPA2. (I-H) Maximal observed RGECO fluorescence intensity and PKCε-EGFP recruitment increases for conditions detailed in (A-H). The dashed line indicates 1.0. (I) Maximal observed normalized RGECO fluorescence intensity and PKCε-EGFP recruitment increases for matching ligand/receptor combinations as detailed in the figure. The dashed line indicates 1.0. Note that that Ca^{2+} transients or PKC recruitment were observed in most cases, as expected. Exemplary images are shown, data in bar graphs are mean, error bars indicate SEM, n-numbers are given in brackets behind experimental conditions and indicate single cell traces. Concentrations indicate the amount of added free GPCR ligand.

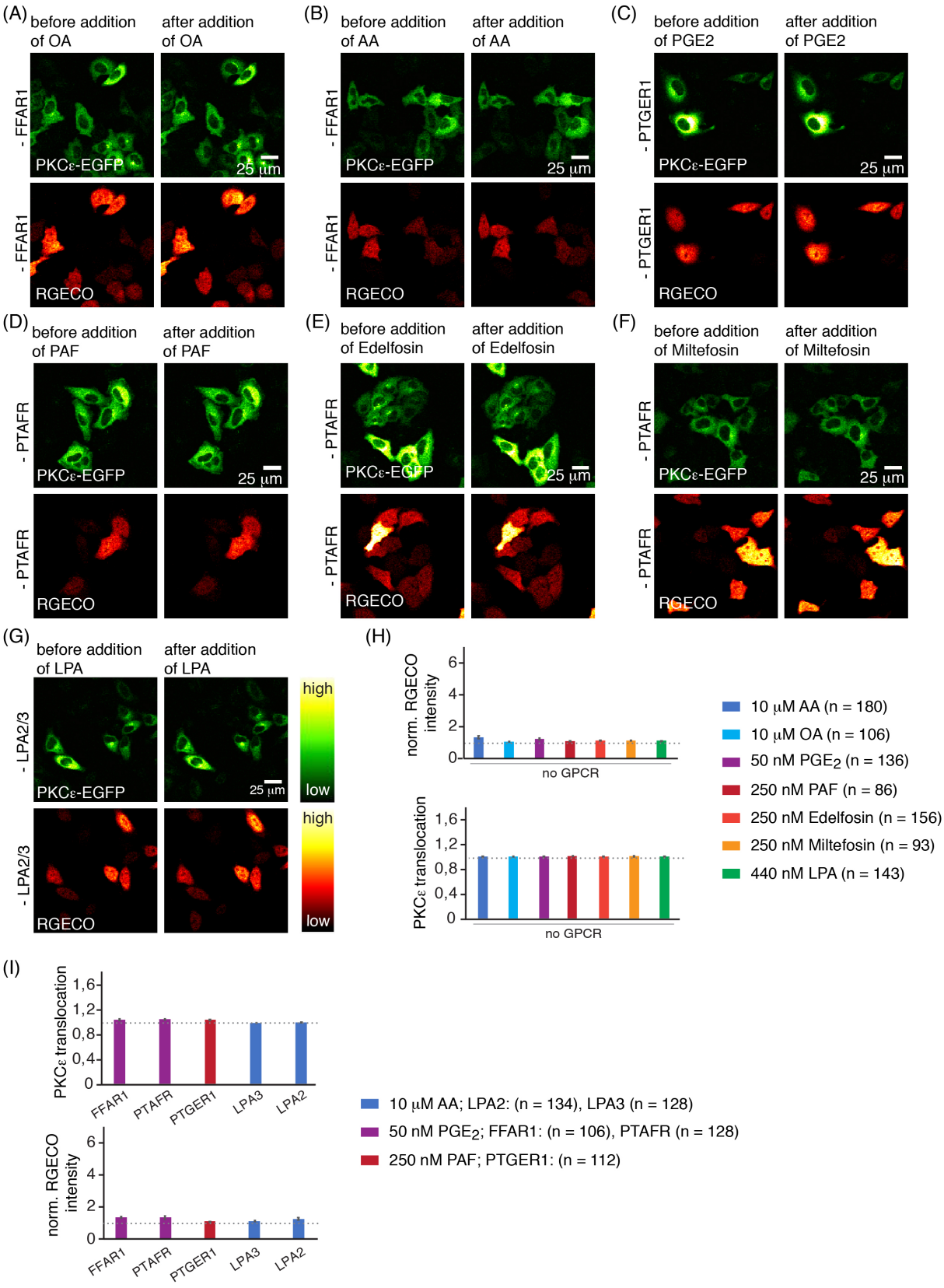

Supplementary Figure S7. Addition of free GPCR ligands to HeLa Kyoto cells without overexpression of GPCRs and addition of mismatched ligands to HeLa Kyoto cells overexpressing GPCRs. (A-B) Cellular localization of PKCε-EGFP and RGECO fluorescence intensity before and after addition of arachidonic acid (AA) (A) and oleic acid (OA) (B) to HeLa Kyoto cells without overexpression of FFAR1. (C) Cellular localization of PKCε-EGFP and RGECO fluorescence intensity before and after addition of prostaglandin E_2 (PGE_2) to HeLa Kyoto cells without overexpression of PTGER1. (D) Cellular localization of PKCε-EGFP and RGECO fluorescence intensity before and after addition of platelet activating factor (PAF) to HeLa Kyoto cells without overexpression of PTAFR. (E) Cellular localization of PKCε-EGFP and RGECO fluorescence intensity before and after addition of edelfosin to HeLa Kyoto cells without overexpression of PTAFR. (F) Cellular localization

of PKCε-EGFP and RGECO fluorescence intensity before and after addition of miltelfosin to HeLa Kyoto cells without overexpression of PTAFR. (G) Cellular localization of PKCε-EGFP and RGECO fluorescence intensity before and after addition of lysophosphatidic acid (LPA) to HeLa Kyoto cells without overexpression of LPA2/3. (H) Maximal observed RGECO fluorescence intensity and PKCε-EGFP recruitment increases for conditions detailed in (A-G). The dashed line indicates 1.0. (I) Maximal observed RGECO fluorescence intensity and PKCε-EGFP recruitment increases for mismatched ligand/receptor combinations as detailed in the figure. The dashed line indicates 1.0. Note that no Ca^{2+} transients or PKC recruitment were observed in any case, as expected. Exemplary images are shown, data in bar graphs are mean, error bars indicate SEM, n-numbers are given in brackets behind experimental conditions and indicate single cell traces. Concentrations indicate the amount of added free GPCR ligand.

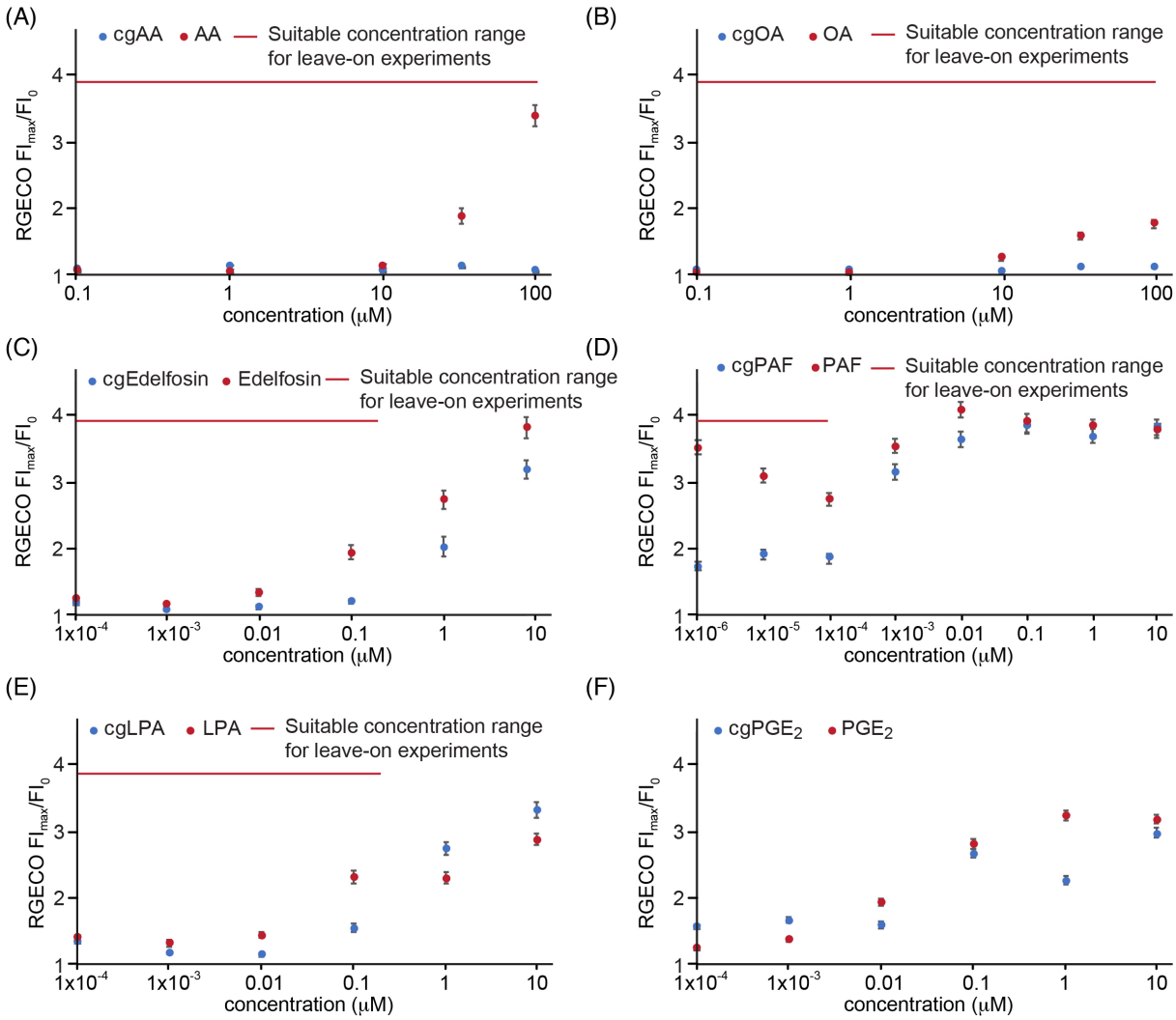

Supplementary Figure S8. Comparison of RGECO responses between additions of caged and free ligands to HeLa Kyoto cells overexpressing the respective GPCRs for assessing the suitability of the synthesized compounds for leave-on experiments. (A)-(F) Comparison of normalized RGECO amplitudes after addition of corresponding free ligands (red) and caged compounds (blue) to HeLa Kyoto cells expressing the corresponding GPCRs. Each data point corresponds to nine individual experiments (three biological replicates, three technical replicates), with each experiment typically corresponding to 30-80 single cells. Data are mean, error bars represent SEM, red bars indicate suitable concentration windows for application of the caged compounds in leave-on experiments for this assay.

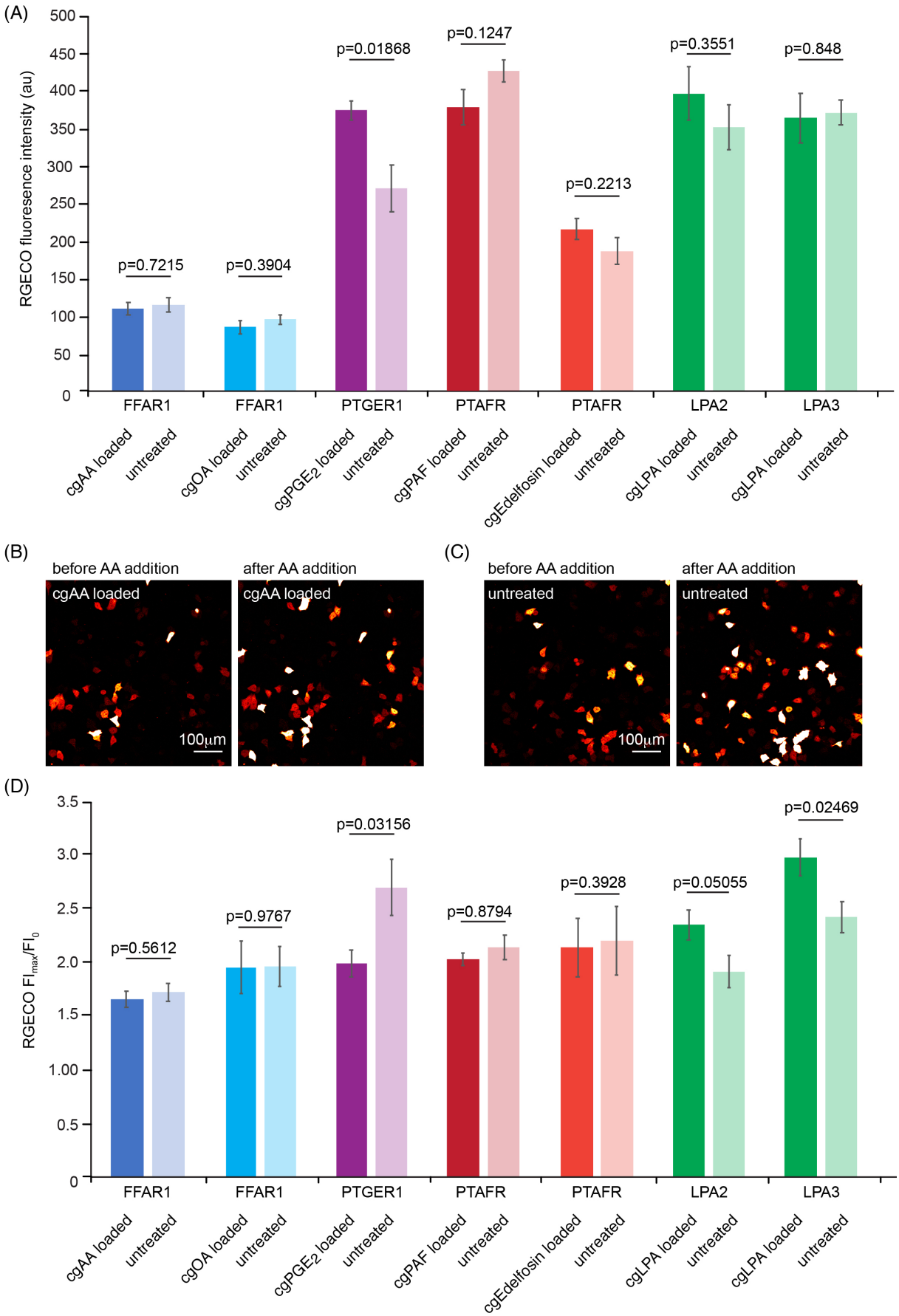

Supplementary Figure S9. Comparison between addition caged and free ligands to HeLa Kyoto cells overexpressing the respective GPCRs for assessing the suitability of the synthesized compounds for wash-off experiments. (A) Comparison of RGECO fluorescence in HeLa Kyoto cells expressing the respective indicated receptor and either loaded with the respective caged compound or untreated. No significant differences were observed with the exception of cells loaded with cgPGE$_2$ (**13**), where slightly higher RGECO fluorescence levels indicate higher resting Ca^{2+} levels. Data are mean (n=6

images), displayed as au, to avoid effects of normalization, p-values were calculated using Welch's unequal variances t-test, error bars represent SEM. (B) Representative images of RGECO fluorescence intensity before and after addition of arachidonic acid (AA) to HeLa Kyoto cells expressing FFAR1 which were loaded with cgAA (**8**). (C) Representative images of RGECO fluorescence intensity before and after addition of arachidonic acid (AA) to untreated HeLa Kyoto cells expressing FFAR1. (D) Comparison of normalized RGECO amplitudes after addition of free ligands to HeLa Kyoto cells expressing the corresponding GPCRs which were either loaded with the respective caged compound (dark colours) or untreated (light colours). Significantly diminished responses were only observed for cgPGE_2 (**13**) loaded cells, in all other cases either similar (statistically not significantly different) or slightly higher responses were observed for cells loaded with the respective caged compounds. Data are mean (n=9 independent experiments), error bars represent SEM and p-values were calculated using Welch's unequal variances t-test. Taken together (all panels), these data indicate that only the presence of cgPGE_2 (**13**) leads to a slight desensitization of the parent receptor, whereas the other compounds do not affect the induced signalling under the conditions used. For details with regard to data analysis, see section 5.3.

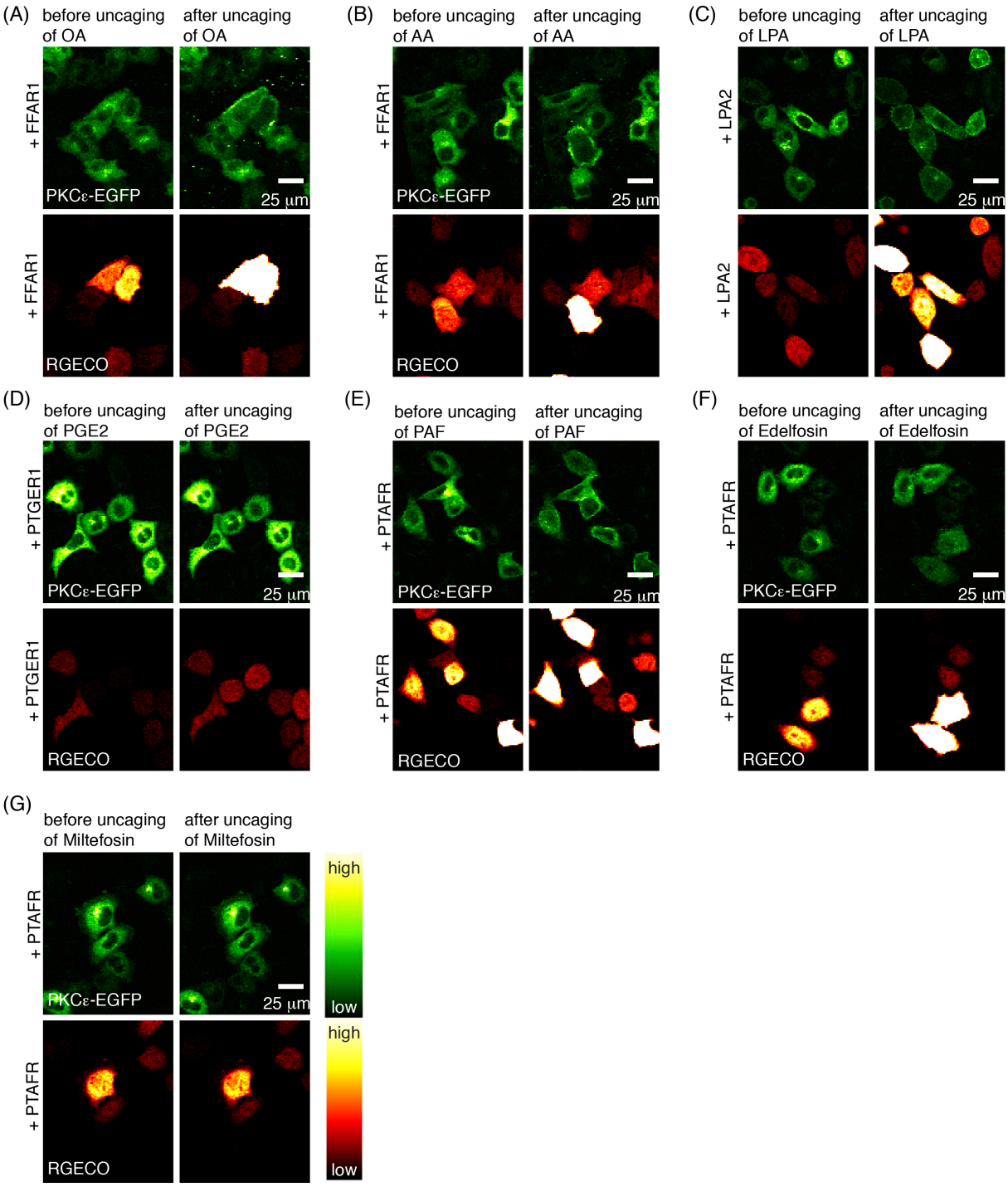

Supplementary Figure S10. Cellular localization of PKCε and RGECO fluorescence intensity before and after uncaging of caged GPCR ligands in cells expressing the respective receptors. (A-B) Cellular localization of PKCε-EGFP and RGECO fluorescence intensity before and after uncaging of arachidonic acid (AA) (A) and oleic acid (OA) (B) in HeLa Kyoto cells overexpressing FFAR1. (C) Cellular localization of PKCε-EGFP and RGECO fluorescence intensity before and after uncaging of lysophosphatidic acid (LPA) in HeLa Kyoto cells overexpressing LPA2. (D) Cellular localization of PKCε-EGFP and RGECO fluorescence intensity before and after uncaging of prostaglandin E_2 (PGE_2) in HeLa Kyoto cells overexpressing PTGER1. (E) Cellular localization of PKCε-EGFP and RGECO fluorescence intensity before and after uncaging of platelet activating factor (PAF) in HeLa Kyoto cells overexpressing PTAFR. (F) Cellular localization of PKCε-EGFP and RGECO fluorescence intensity before and after uncaging of edelfosin in HeLa Kyoto cells overexpressing PTAFR. (G) Cellular localization of PKCε-EGFP and RGECO fluorescence intensity before and after uncaging of miltelfosin in HeLa Kyoto cells overexpressing PTAFR. Exemplary images are shown.

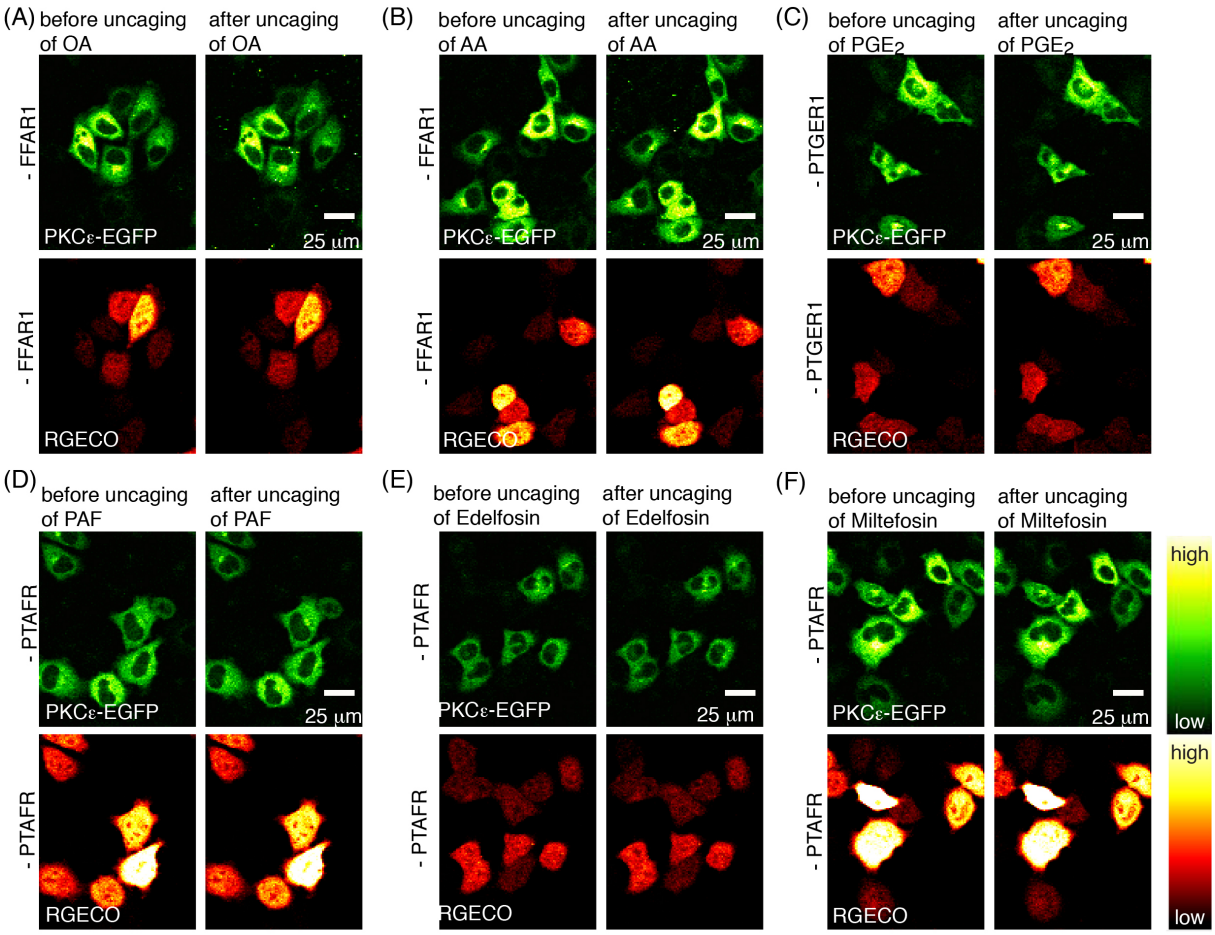

Supplementary Fig. S11. Cellular localization of PKCε and RGECO fluorescence intensity before and after uncaging of caged GPCR ligands without overexpression of GPCRs. (A-B) Cellular localization of PKCε-EGFP and RGECO fluorescence intensity before and after uncaging of arachidonic acid (AA) (A) and oleic acid (OA) (B) in HeLa Kyoto cells without overexpression of FFAR1. (c) Cellular localization of PKCε-EGFP and RGECO fluorescence intensity before and after uncaging of prostaglandin E_2 (PGE_2) in HeLa Kyoto cells without overexpression of PTGER1. (D) Cellular localization of PKCε-EGFP and RGECO fluorescence intensity before and after uncaging of platelet activating factor (PAF) in HeLa Kyoto cells without overexpression of PTAFR. (E) Cellular localization of PKCε-EGFP and RGECO fluorescence intensity before and after uncaging of edelfosin in HeLa Kyoto cells without overexpression of PTAFR. (F) Cellular localization of PKCε-EGFP and RGECO fluorescence intensity before and after uncaging of miltefosin in HeLa Kyoto cells without overexpression of PTAFR. Exemplary images are shown.

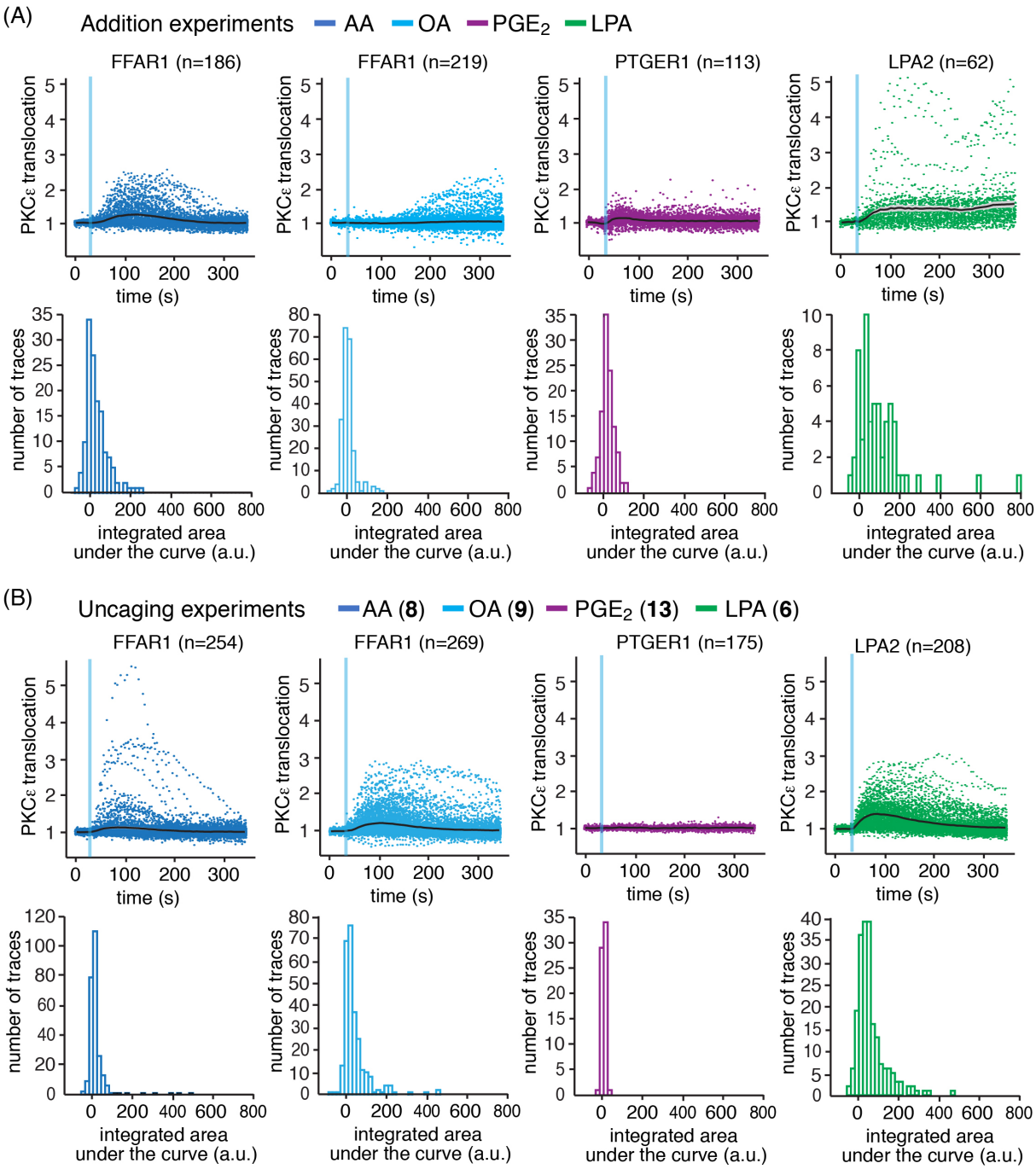

Supplementary Figure S12. Analysis of single cell PKCε recruitment traces of data shown in Fig. 3 and Supplementary Fig. 6, 10. (A) Jitter plots (upper panels) and distribution of integrated areas under single cell traces (lower panels) for PKCε-EGFP recruitment after addition of arachidonic acid (AA) to FFAR1 expressing cells (left panels), oleic acid (OA) to FFAR1 expressing cells (middle left panels), prostaglandin E_2 (PGE_2) to PTGER1 expressing cells (middle right panels) and lysophosphatidic acid (LPA) to LPA2 expressing cells (right panels). Note that for oleic acid (OA) and arachidonic acid (AA) additions, delayed responses were observed when compared to the corresponding uncaging experiments in panels (B) whereas for LPA addition prolonged activation due to continued exposure occurred. (B) Jitter plots (upper panels) and distribution of integrated areas under single cell traces (lower panels) for PKCε-EGFP recruitment after uncaging of arachidonic acid (**8**) in FFAR1 expressing cells (left panels), oleic acid (**9**) in FFAR1 expressing cells (middle left panels), prostaglandin E_2 (**13**) in PTGER1 expressing cells (middle right panels) and lysophosphatidic acid (**6**) in LPA2 expressing cells (right panels). Note that for all compounds responses occur directly after the uncaging event. Black lines in Jitter plots indicate the mean of all single cell traces, shaded areas indicate SEM, blue bars indicate uncaging and addition times. Receptor names above the respective Jitter plot / histogram pairs indicate the overexpressed GPCR for each condition. n-numbers are given in brackets behind receptor names and indicate single cell traces. Concentrations of added free ligands and used for loading of caged

compounds are given in Supplementary Table 2 and 4 and were identical for all experiments during which GPCR induced signaling was monitored.

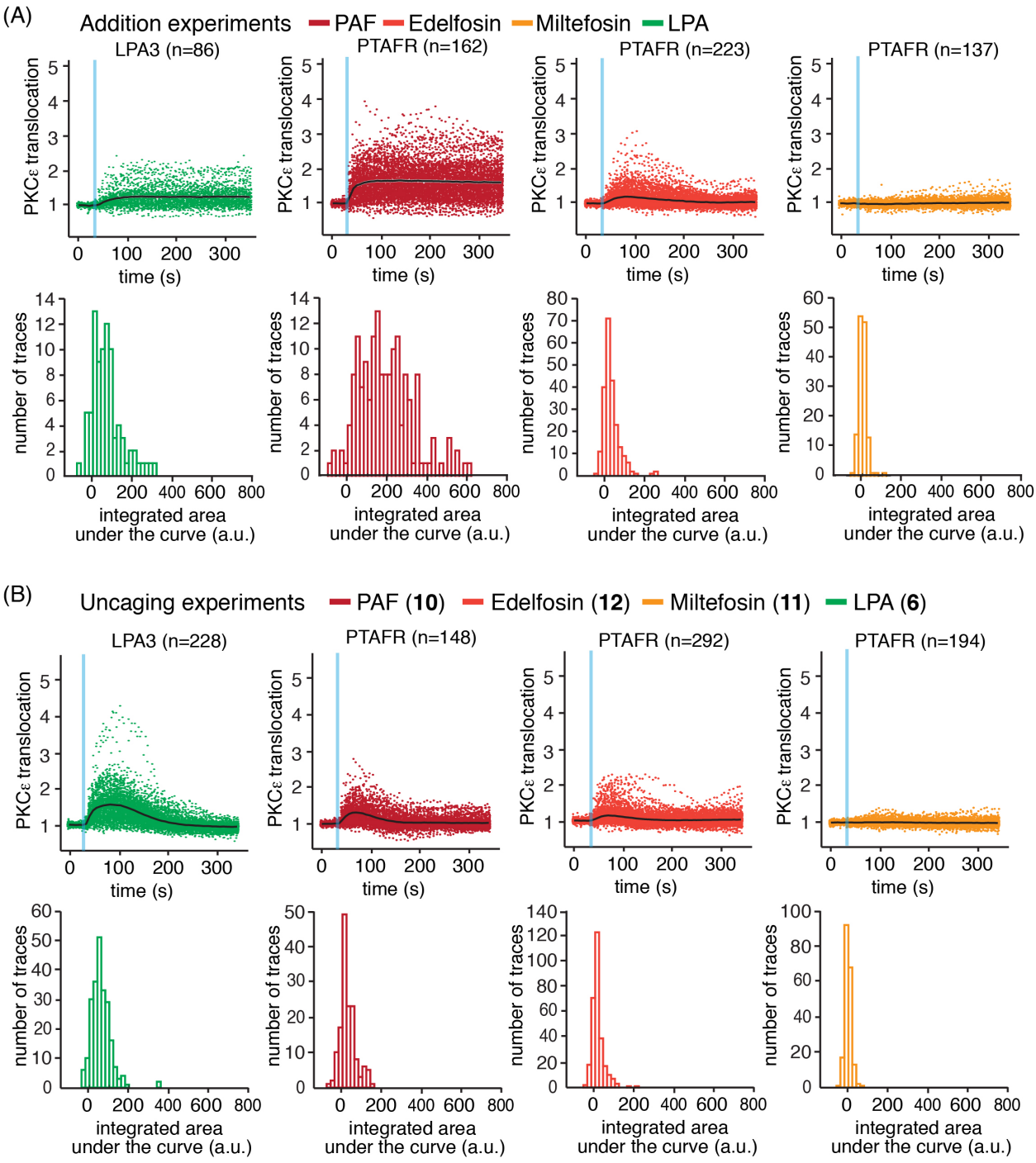

Supplementary Figure S13. | Analysis of single cell PKCε recruitment traces of data shown in Fig. 3 and Supplementary Fig. 6, 10. (A) Jitter plots (upper panels) and distribution of integrated areas under single cell traces (lower panels) for PKCε-EGFP recruitment after addition of lysophosphatidic acid (LPA) to LPA3 expressing cells (left panels), platelet activating factor (PAF) to PTAFR expressing cells (middle left panels), edelfosin to PTAFR expressing cells (middle right panels) and miltefosin to PTAFR expressing cells (right panels). Note that for lysophosphatidic acid (LPA) and platelet activating factor (PAF) prolonged activation due to continued exposure occurred, resulting in a much broader distribution of events when compared to the corresponding uncaging events. (B) Jitter plots (upper panels) and distribution of integrated areas under single cell traces (lower panels) for PKCε-EGFP recruitment after uncaging of lysophosphatidic acid (**6**) in LPA3 expressing cells (left panels), platelet activating factor (**10**) in PTAFR expressing cells (middle left panels), edelfosin (**12**) in PTAFR expressing cells (middle right panels) and miltefosin (**11**) in PTAFR expressing cells (right panels). Note that for all compounds responses occur directly after the uncaging event. Black lines in Jitter plots indicate the mean of all single cell traces, shaded areas indicate SEM, blue bars indicate uncaging and addition times. Receptor names above the respective Jitter plot / histogram pairs indicate the overexpressed GPCR for each condition. n-numbers are given in brackets behind receptor names and indicate single cell traces. Concentrations of added free ligands and used for loading of caged compounds are given in Supplementary Tables 2 and 4 and were identical for all experiments during which GPCR induced signaling was monitored.

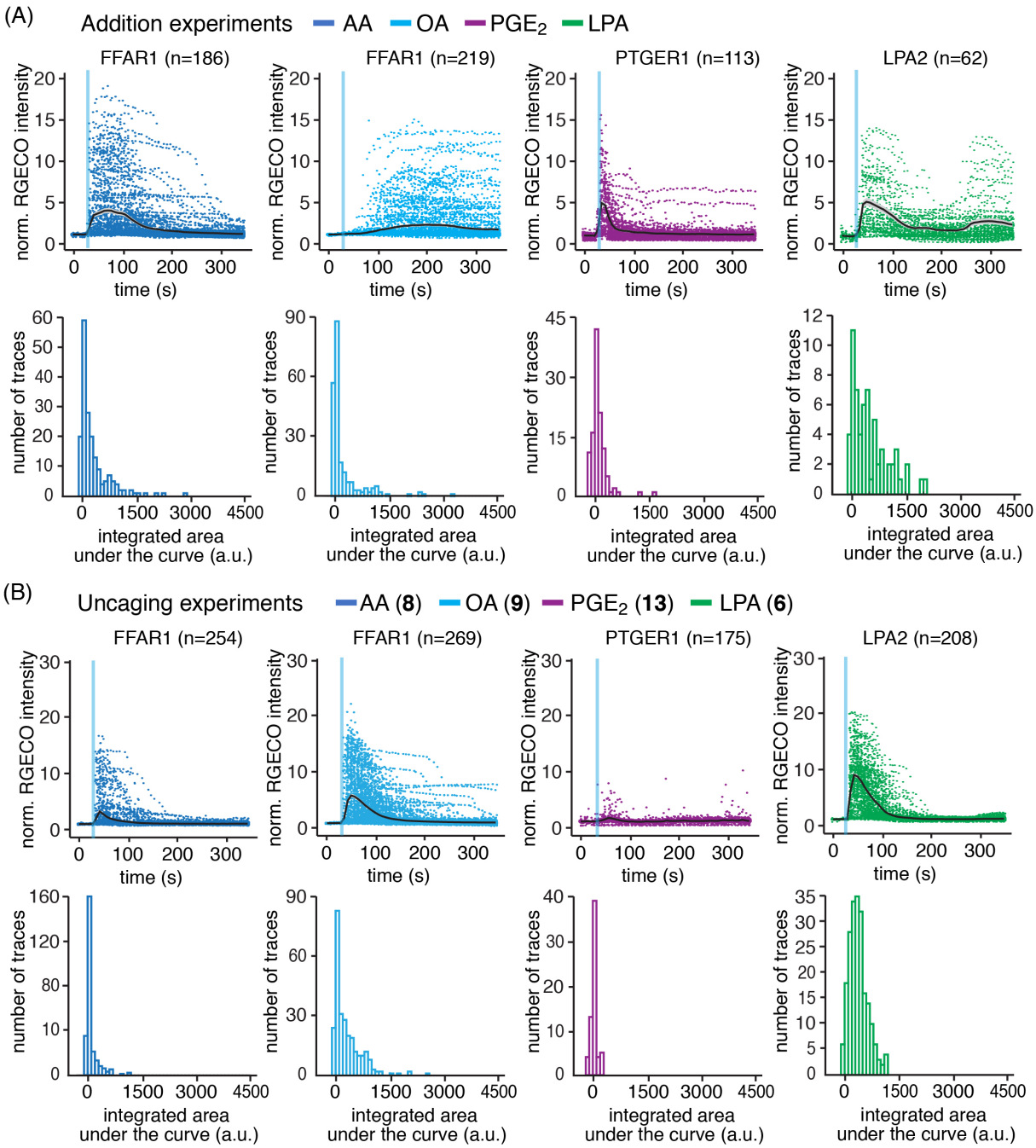

Supplementary Figure S14. Analysis of single cell RGECO traces of data shown in Fig. 3 and Supplementary Fig. 6, 10. Traces were derived from the same cells as PKCε-EGFP recruitment traces displayed in Supplementary Figure 11. (A) Jitter plots (upper panels) and distribution of integrated areas under single cell traces (lower panels) for normalized RGECO fluorescence intensity after addition of arachidonic acid (AA) to FFAR1 expressing cells (left panels), oleic acid (OA) to FFAR1 expressing cells (middle left panels), prostaglandin E_2 (PGE_2) to PTGER1 expressing cells (middle right panels) and lysophosphatidic acid (LPA) to LPA2 expressing cells (right panels). Note that for oleic acid (OA) and arachidonic acid (AA) additions delayed and prolonged responses were observed when compared to the corresponding uncaging experiments in panels (B), whereas for lysophosphatidic acid (LPA) addition secondary calcium transients at later time points were observed. (B) Jitter plots (upper panels) and distribution of integrated areas under single cell traces (lower panels) for normalized RGECO fluorescence intensity after uncaging of arachidonic acid (**8**) in FFAR1 expressing cells (left panels), oleic acid (**9**) in FFAR1 expressing cells (middle left panels), prostaglandin E_2 (**13**) in PTGER1 expressing cells (middle right panels) and lysophosphatidic acid in (**6**) LPA2 expressing cells (right panels). Note that for all compounds responses occur directly after the uncaging event and are more homogenously distributed compared with addition experiments. Black lines in Jitter plots indicate the mean of all single cell traces, shaded areas indicate SEM, blue bars indicate uncaging and addition times. Receptor names above the respective Jitter plot / histogram pairs indicate the overexpressed GPCR for each condition. n-numbers are given in brackets behind receptor names and indicate single cell traces. Concentrations of added free ligands and used for

loading of caged compounds are given in Supplementary Tables 2 and 4 and were identical for all experiments during which GPCR induced signaling was monitored.

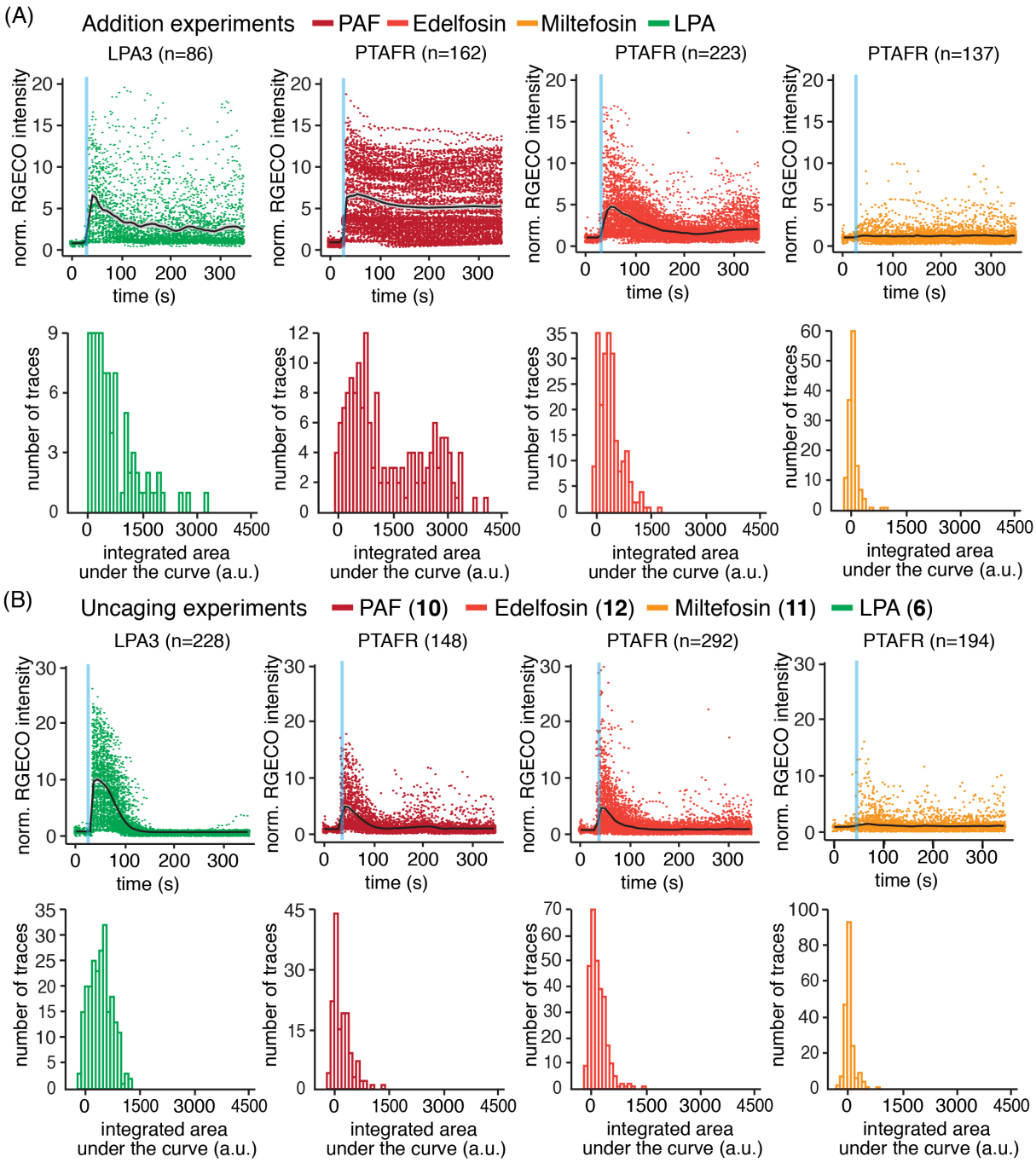

Supplementary Fig. 15. | Analysis of single cell RGECO traces of data shown in Fig. 3 and Supplementary Fig. 6, 10. Traces were derived from the same cells as PKCε-EGFP recruitment traces displayed in Supplementary Fig. 12. (A) Jitter plots (upper panels) and distribution of integrated areas under single cell traces (lower panels) for normalized RGECO fluorescence intensity after addition of lysophosphatidic acid (LPA) to LPA3 expressing cells (left panels), platelet activating factor (PAF) to PTAFR expressing cells (middle left panels), edelfosin to PTAFR expressing cells (middle right panels) and miltefosin to PTAFR expressing cells (right panels). Note that for lysophosphatidic acid (LPA) and platelet activating factor (PAF) additions, prolonged activation due to continued exposure occurred, resulting in a much broader distribution of events when compared to the corresponding uncaging events. (B) Jitter plots (upper panels) and distribution of integrated areas under single cell traces (lower panels) for normalized RGECO fluorescence intensity after uncaging of lysophosphatidic acid (**6**) in LPA3 expressing cells (left panels), platelet activating factor (**10**) in PTAFR expressing cells (middle left panels), edelfosin (**12**) in PTAFR expressing cells (middle right panels) and miltefosin (**11**) in PTAFR expressing cells (right panels). Note that for all compounds responses occur directly after the uncaging event and are more homogenously distributed compared with addition experiments. Black lines in Jitter plots indicate the mean of all single cell traces, shaded areas indicate SEM, blue bars indicate uncaging and addition times. Receptor names above the respective Jitter plot / histogram pairs indicate the overexpressed GPCR for each condition. n-numbers are given in brackets behind receptor names and indicate single cell traces. Concentrations of added free

ligands and used for loading of caged compounds are given in Supplementary Table 2 and 4 and were identical for all experiments during which GPCR induced signaling was monitored.

2. Used equipment and chemicals

All chemicals were obtained from commercial sources (Acros, Sigma-Aldrich, TCI chemicals, Cayman Chemicals, Avanti Polar Lipids, TRC Canada, Carbosynth, Alfa Aesar, Roth, Fluka or Merck) and were used without further purification. Solvents for flash chromatography were obtained from VWR and dry solvents were obtained from Sigma. Deuterated solvents were obtained from Deutero GmbH, Karlsruhe, Germany. TLC was performed on precoated plates of silica gel (Merck, 60 F254) using UV light (254 or 365 nm) or a solution of phosphomolybdic acid in EtOH (10 g phosphomolybdic acid, in 100 ml EtOH) for analysis. Preparative column chromatography was performed using silica gel from Merck, Darmstadt, Germany (silica 60, grain size 0.063-0.200 mm) with a pressure of 1.5 bar. Detailed purification conditions are given for the respective compounds. ^{1}H-, ^{13}C-, ^{31}P- and ^{19}F-NMR-spectra were measured on a 400 MHz Advance^{TM} III HD Nanobay Bruker spectrometer. Chemical shifts of ^{1}H- and ^{13}C-NMR-spectra are referenced indirectly to tetramethylsilane. *J* values are given in Hz and chemical shifts in ppm. Splitting patterns are designated as follows: s, singlet; d, doublet; t, triplet; q, quartet; m, multiplet; b, broad. ^{13}C-NMR-spectra were broadband hydrogen decoupled. Mass spectra (ESI) were recorded using a QExactive instrument (Thermo Fisher Scientific) equipped 660 with a robotic nanoflow ion source. FTMS spectra were acquired with the target mass resolution of m/z 200=140000. The spectra were evaluated using the Xcalibur Qual 662 Browser software.[2]

3. Cell culture and cDNA transfection

The initial characterization of caged lipid performance in cells, loading and localization analyses as well as development and optimization of uncaging protocols and quantification of photoreactions were carried out in HeLa Kyoto cells. Cells were cultured in high-glucose DMEM (31966-021, Life Technologies) supplied with 10% fetal bovine serum (10270-106, LifeTechnologies) and 100 µg ml^{-1} antibiotic Penicillin-Streptomycin (10 000 U/mL, 15140-122, Life Technologies). In preparation to life cell imaging, cells were reversely transfected in either eight-well Lab-Tek microscope dishes (155411, Thermo Scientific) for laser-scanning confocal microscopy (Olympus Fluoview 1000), 24h (to reach 80-100% confluence) before imaging. 60 000 cells (in 450 µl DMEM) were seeded into each well onto a transfection cocktail of 0.4 µl of Lipofectamin 2000 (Thermo Fischer), with 20 µl Opti-MEM (11058-021, Life Technologies) and 230 ng cDNA (PKCe-GFP (75ng) and RGECO (40ng)) with or without the respective GPCR (115 ng). Cells were imaged 24 h after transfection.

GPCR	**ligand**
FFAR1	AA, OA
LPA2	LPA
LPA3	LPA
PTGER1	PGE_2
PTAFR	PAF, EF, MF

Supplementary Table 1. Expressed GPCRs and respective ligands.

4. Compound uptake and intracellular localization

For assessment of compound uptake (Fig. 2B, Supplementary Figure S4, S5), cells were imaged in eight-well Lab-Tek microscope dishes (155411, Thermo Scientific) using an Olympus Fluoview 1000 confocal laser scanning microscope with an Olympus UPlanSApochromat 60x 1.35 oil objective at 37 °C and 5 % CO_2 in imaging buffer (IB) containing 20 mM HEPES,

115 mM NaCl, 1.2 mM $CaCl_2$, 1.2 mM $MgCl_2$, 1.2 mM K_2HPO_4, 10 mM glucose. Microscope settings were adjusted to generate images displaying background fluorescence values slightly larger than zero in order to capture the complete signal stemming from the coumarin dye. For data shown in Figure 2B and Supplementary Figure S4, settings were adjusted to the signal of the individual compounds, for data shown in Supplementary Figure S5, settings were kept identical for all compounds. Coumarin dyes were excited with the 405 nm laser and emitted light was collected between 425 and 475 nm. Images were acquired with the software FV10-ASW 1.7.[2]
Caged compounds were stored as 10 mM DMSO stock solutions at -80 °C and caged compound loading solutions for cellular uptake were generated by appropriate dilution with imaging buffer. HeLa Kyoto cells were grown to 95 % confluence in 8-well Lab-Tek dishes. The medium was removed prior to compound loading, and the cells were washed with imaging buffer (1 x 200 µl per well). Subsequently, the cells were treated with the respective caged compound loading solutions (200 µl per well) for 10 min at room temperature. The loading solution was then removed and the cells washed with imaging buffer (3 x 200 µl per well). All shown compounds were loaded using a final concentration of 10 µM for data shown in Figure 2B and Supplementary Figure S4 and a final concentration of 20 µM for data shown in Supplementary Figure S5.

5. Conditions for time-lapse experiments

Imaging was performed on a dual scanner confocal microscope Olympus Fluoview 1000, with an Olympus UPlanSApochromat 20x oil objective. Microscope settings were adjusted to generate images displaying background fluorescence values slightly larger than zero in order to capture the complete signal stemming from the respective fluorescent proteins. PKCε-EGFP/RGECO were excited with 488/568 nm laser and emitted light was collected at 500–550 nm and 585-685 nm, respectively. Images were acquired with the software FV10-ASW 1.7. All time lapse microscopy experiments were carried out at least in biological triplicates. Each biological replicate contained 2-3 technical replicates, typically resulting in a total number of 50-300 individual single cell traces per condition.

5.1. Addition experiments

Cells were imaged in eight-well Lab-Tek microscope dishes (155411, Thermo Scientific) for laser-scanning confocal microscopy (Olympus Fluoview 1000) at 37 °C and 5% CO_2 in imaging buffer (IB). Cells were placed in imaging buffer 5 min prior to imaging. After an equilibration time of 5 min to 37 °C and 5% CO_2, time lapses were recorded and free ligands were added in 50 µL IB after Frame 5, the final ligand concentrations for all experiments except for Figure S8, S9 (assessment of the concentration dependency of ligand additions, assessment of receptor desensitization by caged compound loading) are summarized in Supplementary Table 2. Ligand concentrations for Figure S9 are summarized in Supplementary Table S3.

free ligand	**addition concentration**
AA	10 µM
OA	10 µM
LPA	440 nM
PGE_2	50 nM
PAF	250 nM
EF	250 nM
MF	250 nM

Supplementary Table 2. Final ligand concentrations for addition experiments for all figures except S8 and S9.

free ligand	addition concentration
AA	100 µM
OA	100 µM
LPA	2 µM
PGE_2	1 µM
PAF	250 nM
EF	250 nM

Supplementary Table 3. Final ligand concentrations for addition experiments figures S8 and S9.

5.2. Uncaging Experiments

Cells were imaged in eight-well Lab-Tek microscope dishes (155411, Thermo Scientific) for laser-scanning confocal microscopy (Olympus Fluoview 1000) at 37 °C and 5% CO_2 in IB. Cells were placed in imaging buffer 5 min prior to imaging. Caged ligands were loaded for 10 min at RT and cells were washed three times with IB after removal of the loading solution. The utilized ligand concentrations are summarized in Supplementary Table 4. After an equilibration time of 5 min to 37 °C and 5% CO_2, time lapses were recorded, where uncaging took place after Frame 5 with the 405 nm laser using a laser power of 40% (equivalent to 0.95 mW at the objective) and a pixel dwell time of 4µs. 405 nm irradiation took place for one frame (total irradiation time: 1.05 s) on a 636 µm-square field of view. This represents a light dose of 0.996 mJ in total or 2.46 nJ/µm^2. The structures of the utilized caged compounds are depicted in Supplementary Scheme 1.

caged compound	loading concentration
cgAA (**8**)	100 µM
cgOA (**9**)	100 µM
cgLPA (**6**)	10 µM
cgPGE_2 (**13**)	100 nM
cgPAF (**10**)	5 nM
cgEF (**12**)	200 nM
cgMF (**11**)	200 nM

Supplementary Table 4. Loading concentrations for uncaging experiments.

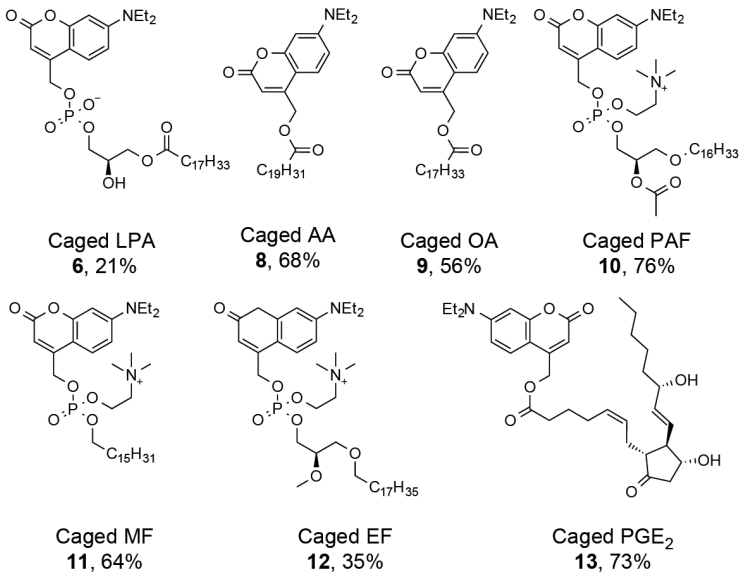

Supplementary Scheme 1. Structures of caged compounds utilized in uncaging assays

5.3. Image analysis and data processing

Images were analyzed using Fiji (http://fiji.sc/Fiji) and the previously reported FluoQ macro[3] to extract kinetic traces. For translocation analysis of PKCε-EGFP using the "translocation efficiency" measure, cells were segmented and the boundary of each cell was used to define a plasma membrane region and a cytosolic region. This information was then used to compute the normalized mean intensity of the defined region and calculating the translocation efficiency as a measure of the extent of PKCε-EGFP recruitment. Translocation efficiency is defined as the ratio between normalized fluorescence intensities at the plasma membrane and in the cytosol. The axis label "PKCε-EGFP-translocation" refers to the translocation efficiency measure in all cases.
For analysis of the Ca^{2+} signal typically RGECO fluorescence intensities of individual cells were measured. Data are displayed in all figures in a normalized (respective to baseline values prior to stimulation) fashion except for Figure S9A where raw data are shown in arbitrary units to better illustrate variability between experimental conditions. For data displayed in Figure S9, whole field of view intensities were determined to better capture variation between experiments. Time series data were analyzed using the software R and RStudio.

$$Translocation\ efficiency = \frac{{}^{FI}/_{FI_0}\,(membrane)}{{}^{FI}/_{FI_0}\,(cytosol)}$$

Integrated RGECO and PKCε-EGFP-translocation efficiency values were computed using the trapz function of the MATLAB software (Figure S12-15). Integrated areas were defined as the area between the normalized curve and a parallel line to the y-axis with a value of 1. This procedure results in a value of approximately 0 for time traces that do not show an effect after stimulation, stronger effects are characterized by higher positive values.

6. Photo liberation HPLC assay for new compounds

A semi-preparative gradient RP-HPLC Knauer Azura system with a Eurosphere II 100-5 C_4 column was used to analyse photoreaction mixtures. Solvents were chosen according to the molecule to be analysed. The uncaged and caged derivatives eluted during the same HPLC run under the same conditions (shown below) with different R_t and baseline separation.
First, the retention times R_t of the free parent molecules (not shown) and the caged derivatives were determined (see Supplementary Fig. 3, panels PAF-0s and OHOA-0s) and Supplementary Table 6). 20 µl of 10 mM solutions of the compounds in DMSO were diluted with 130 µl MeOH and injected before the runs were started. For bulk uncaging a 1000 W Mercury-Xenon lamp with a 335 nm high pass filter was used. For uncaging, 20 µl of 10 mM solution of the compounds in DMSO were diluted with 130 µl MeOH in a 250 µl Eppendorf tube and placed in a stand approx. 20 cm away from the light source. For each compound the sample was illuminated for 15s, 60s and 300s. For caged carboxylates an additional sample was illuminated for 600s. Directly after illumination, the samples were analysed by semi-preparative RP-HPLC (Supplementary Tables 5 & 6). The runs of the samples that were illuminated for 300s were fractionated and the fraction containing uncaged compounds (R_t matching the R_t of the respective free parent molecules) were analysed by HRMS. The detected masses corresponded to the calculated masses of the free parent compounds (Supplementary Table 7).

6.1. Conditions for compounds 5,7,9,10,11,12,13,14

Solvent A (750 ml MeOH; 250 ml water; 4 ml acetic acid); Solvent B (500 ml 2-propanol; 300 ml acetonitrile; 200 ml tetrahydrofuran; 4 ml acetic acid). Linear gradients were applied

for all changes in elution conditions. The flowrate for caged DOPA was 1 ml/min lower at every timepoint.

time (min)	% of solvent B	flowrate (ml/min)
0	0	4
2	0	4
11	100	5
12	100	6
15	100	6
16	100	4
17	0	4
20	0	4

Supplementary Table 5. HPLC gradient used for compounds 5,7,9,10,11,12,13,14.

6.2. Conditions for caged N-acetyl neuraminic acid

Solvent A (Water with 0.01 % TFA); Solvent B (MeOH with 0.01 % TFA). Linear gradients were applied for all changes in elution conditions.

time (min)	% of solvent B	flowrate (ml/min)
0	0	3
2	0	3
12	100	3
16	100	3
16.5	0	3
20	0	3

Supplementary Table 6. HPLC gradient used for compound 15.

compound	R_t (min) caged ELSD/DAD	R_t (min) uncaged ELSD	exact mass (Da) parent compound calculated	exact mass (Da) liberated compound found	complete uncaging after (s)
cgPOPC **5**	8.8	11.1	759.58	760.580 $[M+H]^+$	60
cgDOPA **7**	11.7	12.0	700.50	699.502 $[M-H]^-$	300
cgOA **9**	9.4	10.1	282.26	281.247 $[M-H]^-$	300
cgPAF **10**	7.3	9.1	523.36	524.368 $[M+H]^+$	60
cgMF **11**	6.5	8.3	407.32	408.321 $[M+H]^+$	60
cgEF **12**	7.7	9.8	523.40	524.404 $[M+H]^+$	60
cgPGE_2 **13**	6.7	4.0	352.22	351.215 $[M-H]^-$	300
cgOHOA **14**	9.8	9.2	298.25	297.241 $[M-H]^-$	300
cgNANA **15**	8.4	4.2	309.11	310.111 $[M+H]^+$	600

Supplementary Table 7. Summary and confirmation of photo liberation of free parent molecules. Retention times of the caged molecules prior to irradiation with a 1000 W Mercury-Xenon (335 nm high-pass filter) are displayed as

well as the retention times of the peaks detected after irradiation. The latter match the retention times of the respective parent molecules. Molecular identity after uncaging was confirmed by HR-MS.

7. Photochemical characterization of new compounds

Absorbance and fluorescence were measured using a TECAN Spark® 20M Multimode microplate reader (Plates: Microplate, 384 Well, PS, small volume, lobase, med. binding, black, µCLEAR®). For absorbance, the detection range was set to 200-500 nm, the spectral resolution to 2 nm and the averaging time to 0.1 s. The path length of the cuvette was 0.1989 cm (*d*), baseline correction was carried out by subtraction of the background signal of an ethanol sample. Extinction coefficients were determined by plotting the maxima of a serial dilution, using a linear fit to determine the slope (*m*) and calculated as following:

$$\varepsilon = \frac{m}{d} * 1000$$

Emission spectra were recorded with 5-nm resolution. Excitation wavelength for all coumarin derivatives was 380 nm and emission collection at 400-600 nm, with a step size of 2 nm, and 40 µs integration. All spectra were background corrected for ethanol.
Quantum Yields (QYs) were calculated as following:

$$QY = QY_{ref} \frac{\eta^2}{\eta_{ref}^2} \frac{A_{ref}}{A} \frac{I}{I_{ref}}$$

where QY_{ref} is the QY of the reference compound (cg AA, QY = 0.34)[1], η is the refractive index of the solvent (ethanol for all samples and the reference), A is the absorbance at the excitation wavelength, I is the integrated fluorescence intensity.

8. Comparison of activated coumarin reagents

The developed method using the coumarin triflate reagent **1** was compared to the respective coumarin mesylate **2** and diazo **3** reagents in reactions with POPC and PAF. Method A represents the conditions optimized for the triflate reagent, whereas method B closely mirrors previously reported (ref 25a in the main text) conditions for the generation of coumarinyl phosphoesters using the diazo reagent **3**. Chloroform was added in each case to ensure lipid solubility. Conversion was monitored by analysing reaction mixtures by RP-HPLC. Results are summarized in Figure S1.

POPC Method A:

Triflate reagent **1**
25 µmol (6.2 mg, 1eq) 7-(diethylamino)-4-(hydroxymethyl)-coumarin were dissolved in 1 ml dry DCM with 50 µl DIEA and cooled with an ice bath. 84 µl of a 1:20 dilution of Tf_2O in dry DCM were added and after 2 min the resulting triflate reagent was transferred into an ice-cold solution of 25 µmol (19 mg, 1eq) POPC in 1 ml chloroform. The reaction mixture was slowly allowed to reach room temperature. After 3 h, a 100 µl sample of the reaction mix was analysed by HPLC.
Mesylate **2**
25 µmol (19 mg, 1eq) POPC and 8.9 mg **2** were dissolved in 1 ml dry chloroform and 1 ml dry DCM with 50 µl DIEA and cooled with an ice bath. The reaction mixture was slowly allowed to reach room temperature. After 3 h, a 100 µl sample of the reaction mix was analysed by HPLC.

Diazo coumarin **3**
25 µmol (19 mg, 1eq) POPC and 6.4 mg **3** were dissolved in 1 ml dry chloroform and 1 ml dry DCM with 50 µl DIEA and cooled with an ice bath. The reaction mixture was slowly allowed to reach room temperature. After 3 h, a 100 µl sample of the reaction mix was analysed by HPLC.

POPC Method B:

Triflate reagent **1**
25 µmol (6.2 mg, 1eq) 7-(diethylamino)-4-(hydroxymethyl)-coumarin were dissolved in 1 ml dry chloroform with 50 µl DIEA and cooled with an ice bath. 84 µl of a 1:20 dilution of Tf_2O in dry DCM were added and after 2 min the resulting triflate reagent was transferred into a solution of 25 µmol (19 mg, 1eq) POPC in 1ml of a 1:1 mix of dry DMSO and dry acetonitrile. The reaction mixture was heated to 60 ºC. After 20 h, a 100 µl sample of the reaction mix was analysed by HPLC.
Mesylate **2**
25 µmol (19 mg, 1eq) POPC and 8.9 mg **2** were dissolved in 1 ml dry chloroform and 1 ml of a 1:1 mix of dry DMSO and dry acetonitrile with 50 µl DIEA and heated to 60 ºC. After 20 h, a 100 µl sample of the reaction mix was analysed by HPLC.
Diazo coumarin **3**
25 µmol (19 mg, 1eq) POPC and 6.4 mg **3** were dissolved in 1 ml dry chloroform and 1 ml of a 1:1 mix of dry DMSO and dry acetonitrile with 50 µl DIEA and heated to 60 ºC. After 20 h, a 100 µl sample of the reaction mix was analysed by HPLC.

PAF Method A:

Triflate reagent **1**
25 µmol (6.2 mg, 1eq) 7-(diethylamino)-4-(hydroxymethyl)-coumarin were dissolved in 1 ml dry DCM with 50 µl DIEA and cooled with an ice bath. 84 µl of a 1:20 dilution of Tf_2O in dry DCM were added and after 2 min the resulting triflate reagent was transferred into an ice-cold solution of 25 µmol (13.1 mg, 1eq) PAF in 1 ml dry chloroform. The reaction mixture was slowly allowed to reach room temperature. After 3 h, a 100 µl sample of the reaction mix was analysed by HPLC.

Mesylate **2**
25 µmol (13.1 mg, 1eq) PAF and 8.9 mg **2** were dissolved in 1ml dry chloroform and 1 ml dry DCM with 50 µl DIEA and cooled with an ice bath. The reaction mixture was slowly allowed to reach room temperature. After 3 h, a 100 µl sample of the reaction mix was analysed by HPLC.
Diazo coumarin **3**
25 µmol (13.1 mg, 1eq) PAF and 6.4 mg **3** were dissolved in 1ml dry chloroform and 1 ml dry DCM with 50 µl DIEA and cooled on an ice bath. The reaction mixture was slowly allowed to reach room temperature. After 3 h, a 100 µl sample of the reaction mix was analysed by HPLC.

PAF Method B:

Triflate reagent **1**
25 µmol (6.2 mg, 1eq) 7-(diethylamino)-4-(hydroxymethyl)-coumarin were dissolved in 1 ml dry chloroform with 50 µl DIEA and cooled with an ice bath. 84 µl of a 1:20 dilution of Tf_2O in DCM were added and after 2 min the resulting triflate reagent was transferred into a solution of 25 µmol (13.1 mg, 1eq) PAF in 1ml of a 1:1 mix of dry DMSO and dry acetonitrile. The

reaction mixture was heated to 60 ºC. After 20 h, a 100 µl sample of the reaction mix was analysed by HPLC.

Mesylate **2**

25 µmol (13.1 mg, 1eq) PAF and 8.9 mg **2** were dissolved in 1ml dry chloroform and 1 ml of a 1:1 mix of dry DMSO and dry acetonitrile with 50 µl DIEA and heated to 60 ºC. After 20 h, a 100 µl sample of the reaction mix was analysed by HPLC.

Diazo coumarin **3**

25 µmol (13.1 mg, 1eq) PAF and 6.4 mg **3** were dissolved in 1ml dry chloroform and 1 ml of a 1:1 mix of dry DMSO and dry acetonitrile with 50 µl DIEA and heated to 60 ºC. After 20 h, a 100 µl sample of the reaction mix was analysed by HPLC.

For semipreparative RP-HPLC, the following solvent system was used on a Knauer Azura system equipped with a Knauer Eurospher II C_4 column (250 x 8 mm, 5 µm particle size): Solvent A: 750 ml MeOH, 250 ml water and 4 ml AcOH; solvent B: 500 ml 2-propanol, 200 THF, 300 MeCN and 4 ml AcOH. The utilized gradient is shown in Supplementary Table 7. The volatile content of the 100 µl samples collected from individual reactions was removed under reduced pressure and the residues were dissolved in 1 ml MeOH. Insoluble material was removed by 3 min centrifugation with 10000 rpm. Molecular identities of cgPAF (**10**, retention times 6.9 min, found mass: $[M]^+$ 753.482) and cgPOPC (**5**, retention times 8.9 min, found mass: $[M]^+$ 989.695) were confirmed by HR-MS. Results are shown in Figure 1 and Supplementary Figure S1.

Time (min)	% of solvent B	Flowrate (ml/min)
0	0	3.5
2	0	3.5
11	100	4.5
12	100	6
15	100	6
16	100	3.5
17	0	3.5
20	0	3.5

Supplementary Table 7. HPLC gradient used for the comparison of different reaction methods.

9. Synthetic procedures

9.1. Synthesis of 7-(diethylamino)-4-(hydroxymethyl)-coumarin, coumarin mesylate 2 and diazo derivative 3

These compounds were synthesized according to literature.[4-6]

9.2. Caged POPC, cg POPC, 5

2-((((7-(diethylamino)-2-oxo-2H-chromen-4-yl)methoxy)((R)-2-(oleoyloxy)-3 (palmitoyloxy) propoxy)phosphoryl)oxy)-N,N,N-trimethylethan-1-aminium

To form the coumarin triflate reagent **1**, a solution of Tf_2O (24 µl, 142 µmol, 1.1 equiv., 1:10 dilution in DCM) was added to an ice-cold solution of 7-diethylamino 4-hydroxymethyl coumarin (35 mg, 142 µmol, 1.1 equiv.) and DIEA (200 µl, 1.15 mmol) in 1.5 ml dry DCM under inert conditions in an ice bath. After 2 minutes the resulting activated coumarin solution was transferred into a precooled flask with a solution of POPC (100 mg, 132 µmol, 1 eq) in 1.5 ml dry $CHCl_3$. After 30 minutes a freshly prepared solution of the activated coumarin triflate reagent (0.6 equiv.) was added to the reaction mixture and after 90 min another 0.3 equivalents. The reaction mixture was then slowly allowed to reach room temperature while stirring was continued for 3 h. The reaction was quenched by adding 1 ml MeOH and the solvents were removed under reduced pressure. The crude was dissolved in methanol and insoluble material was removed by centrifugation. The product was purified by preparative RP-HPLC (solvent A: 25 % water, 25 % 2-propanol, 50 % MeOH and 0.01 % TFA; solvent B: 60 % 2-propanol, 15 % THF, 25 % MeCN and 0.01 % TFA; 0-3 min 0 % B increasing linearly to 100 % B at 20 min, holding 100 % B until 25 min; constant flowrate 20ml/min) on a Knauer Azura system with a NUCLEODUR® C18 Pyramid column. **5** eluted at 18-19 min. 65 mg of a yellow solid were obtained (66 µmol, 50 %).

HR-MS (ESI positive) m/z found: calculated for $C_{56}H_{98}N_2O_{10}P^+$: 989.6954; found: 989.693 $[M]^+$

^{1}H NMR (400 MHz, MeOD) δ = 7.46 (dd, *J* = 9.1, 5.2 Hz, 1H), 6.75 (dd, *J* = 9.1, 2.6 Hz, 1H), 6.56 (s, 1H), 6.16 (d, *J* = 7.1 Hz, 1H), 5.44 – 5.27 (m, 5H), 4.65 (m_c, 2H), 4.46 – 4.14 (m, 4H), 3.84 – 3.76 (m, 2H), 3.48 (q, *J* = 7.1 Hz, 4H), 3.24 (s, 9H), 2.38 – 2.25 (m, 4H), 2.08 – 1.95 (m, 4H), 1.66 – 1.51 (m, 4H), 1.40 – 1.17 (m, 54H), 0.90 (t, *J* = 6.6 Hz, 6H) ppm. Two diastereomers present.

^{13}C carbon resonances that exhibit coupling patterns due to ^{31}P-^{13}C couplings and overlapping peaks due to the presence of two diastereomers, as well as overlapping peaks in the aliphatic regions are marked as multiplets (m) in the peak list and given as a range.

^{13}C NMR (101 MHz, MeOD) δ = 174.72, 174.33, 174.25, 163.91, 157.60, 152.57, 151.74-151.64 (m), 130.92, 130.73, 126.06, 110.49, 106.55, 106.37, 106.34, 98.41, 71.09- 70.91 (m), 68.14, 68.09, 66.85-66.69 (m), 63.12, 63.07, 62.77, 54.58- 54.51(m), 45.70, 35.00-34.98 (m), 34.83, 33.11, 33.09, 30.87- 30.81 (m), 30.68-30.65 (m), 30.52-30.49 (m), 30.39-30.36 (m), 30.26-30.17 (m), 28.18, 26.00-25.97 (m), 23.77, 14.52-14.50 (m), 12.79 ppm.

^{31}P NMR (162 MHz, $CDCl_3$) δ = -1.57, -1.66 ppm.

9.3. Caged LPA, cg LPA, 6

(2R)-3-((((7-(diethylamino)-2-oxo-2H-chromen-4-yl)methoxy)(hydroxy)phosphoryl)oxy)-2-hydroxypropyl oleate.

To form the coumarin triflate reagent **1**, a solution of Tf_2O (36.3 µl, 216 µmol, 1.1 eq, 1:10 dilution in DCM) was added to an ice-cold solution of 7-diethylamino 4-hydroxymethyl coumarin (53.4 mg, 216 µmol, 1.1 equiv.) and DIEA (200 µl, 1.15 mmol) in 1.5 ml dry DCM under inert conditions in an ice bath. After 2 minutes the resulting activated coumarin solution was transferred into a precooled flask with a solution of 1-oleoyl-LPA in 3.6 ml chloroform (90 mg, 196 µmol, 1.0 equiv.). After 120 minutes a freshly prepared solution of the activated coumarin (0.6 equiv.) was added and the reaction mixture was allowed to slowly reach room temperature. After 4 hours the reaction was quenched by adding 1 ml MeOH and the solvents were removed under reduced pressure. The crude product was purified by flash column chromatography (3 times, 10-20 % MeOH in DCM) to afford 27 mg of a yellow solid (40.5 µmol, 21 %).

HR-MS (ESI negative) m/z found: calculated for $C_{35}H_{56}NO_9P$: 665.3693; found: 664.351 $[M-H]^-$

^1H NMR (400 MHz, MeOD) δ = 7.44 (d, J = 9.0 Hz, 1H), 6.71 (dd, J = 9.0, 2.6 Hz, 1H), 6.50 (d, J = 2.6 Hz, 1H), 6.24 (s, 1H), 5.39 – 5.29 (m, 2H), 5.09 (dd, J = 6.1, 1.4 Hz, 2H), 4.14 (m_c, 2H), 4.01 – 3.90 (m, 3H), 3.46 (q, J = 7.0 Hz, 4H), 2.27 (t, J = 7.5 Hz, 2H), 2.09 – 1.94 (m, 4H), 1.60 – 1.47 (m, 2H), 1.38 – 1.16 (m, 27H), 0.89 (t, J = 6.7 Hz, 3H) ppm.

^{13}C carbon resonances that exhibit coupling patterns due to ^{31}P-^{13}C couplings, as well as overlapping peaks in the aliphatic regions are marked as multiplets (m) in the peak list and given as a range.

^{13}C NMR (101 MHz, MeOD) δ = 175.26, 164.65, 157.36, 154.88-154.80 (m), 152.34, 130.86, 130.78, 125.96, 110.37, 107.16, 105.63, 98.24, 69.75-69.67 (m), 67.63-67.58 (m), 65.93, 64.14-64.13 (m), 45.62, 34.86, 33.04, 30.83, 30.78, 30.59, 30.42, 30.32, 30.27, 30.17, 28.12, 25.94, 23.72, 14.44, 12.79 ppm.

^{31}P NMR (162 MHz, MeOD) δ = -1.39 ppm.

9.4. Caged DOPA, cg DOPA, 7

(2R)-3-((((7-(diethylamino)-2-oxo-2H-chromen-4-yl)methoxy)(hydroxy)phosphoryl)oxy) propane-1,2-diyl dioleate.

To form the coumarin triflate reagent **1**, a solution of Tf_2O (16.5 µl, 98 µmol, 0.71 equiv., 1:10 dilution in DCM) was added to an ice-cold solution of 7-diethylamino 4-hydroxymethyl coumarin (24 mg, 97 µmol, 0.71 equiv.) and DIEA (200 µl, 1.15 mmol) in 1.5 ml dry DCM under inert conditions in an ice bath. After 2 minutes the resulting activated coumarin solution was transferred into a precooled flask with a solution of DOPA in 3 ml dry chloroform (100 mg, 138 µmol, 1.0 equiv.). After 120 minutes a freshly prepared solution of the activated coumarin (0.71 equiv.) was added and the reaction mixture was allowed to slowly reach room temperature. After 3 hours the reaction was quenched by adding 1 ml MeOH and subsequently all volatiles were removed under reduced pressure. The crude product was dissolved in MeOH and purified by preparative gradient RP-HPLC using a Knauer Azura system with a NUCLEODUR® C18 Pyramid column. With a constant flowrate of 15 ml/min, 100 % solvent A (500 ml water, 250 ml MeOH, 250 ml 2-propanol with 0.01 % TFA and 5 mM ammonium formate) was kept for 3 min. Using a linear gradient reaching 50 % solvent B (2-propanol with 0.01 % TFA and 5 mM ammonium formate) after 10 min, 100 % B after 26 min, holding 100 % B until 29 min, the product eluted after 21 min. After subsequent flash column chromatography (10-20% MeOH in DCM) 25 mg of a yellow solid were obtained (27 µmol, 20 %).

HR-MS (ESI negative) m/z found: calculated for $C_{53}H_{88}NO_{10}P$: 929.6146; found: 928.611 $[M-H]^-$

^1H NMR (400 MHz, DMSO) δ = 7.42 (d, *J* = 9.0 Hz, 1H), 6.65 (dd, *J* = 9.1, 2.5 Hz, 1H), 6.50 (d, *J* = 2.5 Hz, 1H), 6.06 (s, 1H), 5.34 – 5.26 (m, 4H), 5.08 – 5.01 (m, 1H), 4.86 – 4.77 (m, 2H), 4.27 (dd, *J* = 12.0, 3.2 Hz, 1H), 4.08 (dd, *J* = 12.0, 6.8 Hz, 1H), 3.41 (q, *J* = 7.0 Hz, 9H, overlapping with water peak), 2.26 – 2.12 (m, 4H), 2.00-1.90 (m, 8H), 1.50 – 1.38 (m, 4H), 1.29 – 1.08 (m, 46H), 0.84 (t, *J* = 6.3 Hz, 6H) ppm.

^{13}C carbon resonances that exhibit coupling patterns due to ^{31}P-^{13}C couplings, as well as overlapping peaks in the aliphatic regions are marked as multiplets (m) in the peak list and given as a range.

^{13}C NMR (101 MHz, DMSO) δ = 172.95-172.66 (m), 161.42, 156.13, 154.40, 150.64, 130.06, 125.49, 109.01, 106.09, 105.07, 97.25, 71.09-71.01 (m), 63.15, 62.71, 62.50, 44.42, 34.03, 33.84, 31.75, 29.56-27.03 (m), 24.89-24.86(m), 14.39, 12.78 ppm.

^{31}P NMR (162 MHz, DMSO) δ = -1.30 ppm.

9.5. Caged arachidonic acid, cg AA, 8

(7-(diethylamino)-2-oxo-2H-chromen-4-yl)methyl arachidonate.

To form the coumarin triflate reagent **1**, a solution of Tf_2O (27.6 µl, 164 µmol, 1.0 equiv., 1:10 dilution in DCM) was added to an ice-cold solution of 7-diethylamino 4-hydroxymethyl coumarin (42 mg, 170 µmol, 1.04 equiv.) and DIEA (100 µl, 0.59 mmol) in 2 ml dry DCM under inert conditions in an ice bath. After 2 minutes the resulting activated coumarin solution was transferred into a precooled flask with a solution of arachidonic acid in 1.5 ml chloroform (50 mg, 163 µmol, 1.0 equiv.). After 2 hours the reaction was quenched by adding 1 ml MeOH, followed by the removal of all volatiles under reduced pressure. The crude product was purified by flash column chromatography (1 % MeOH in DCM) to yield 60 mg of a yellow solid (112 µmol, 68 %).

HR-MS (ESI positive) m/z found: calculated for $C_{34}H_{47}NO_4$: 533.3505; found: 534.3611 $[M+H]^+$

^1H NMR (400 MHz, $CDCl_3$) δ = 7.22 (d, J = 9.0 Hz, 1H), 6.51 (dd, J = 9.0, 2.6 Hz, 1H), 6.45 (d, J = 2.6 Hz, 1H), 6.06 (s, 1H), 5.42 – 5.20 (m, 8H), 5.15 (s, 2H), 3.35 (q, J = 7.1 Hz, 4H), 2.83 – 2.68 (m, 6H), 2.39 (t, J = 7.6 Hz, 2H), 2.09 (dt, J1,2 = 7.1 Hz, 2H), 1.98 (dt, J1,2 = 6.9 Hz, 2H), 1.71 (tt, J1,2 = 7.5 Hz, 2H), 1.34 – 1.18 (m, 6H), 1.14 (t, J = 7.1 Hz, 6H), 0.82 (t, J = 6.8 Hz, 3H) ppm.

Overlapping peaks in the aliphatic regions are marked as multiplets (m) in the peak list and given as a range.

^{13}C NMR (101 MHz, $CDCl_3$) δ = 172.83, 161.83, 156.26, 150.60, 149.46, 130.49, 129.14, 128.66, 128.59, 128.28, 128.07, 127.85, 127.54, 124.38, 108.72, 106.55, 106.13, 97.96, 61.21, 44.82, 33.46, 31.52, 29.33, 27.22, 26.52, 25.64 (m), 24.68, 22.58, 14.07, 12.42 ppm.

9.6. Caged oleic acid, cg OA, 9

(7-(diethylamino)-2-oxo-2H-chromen-4-yl)methyl oleate.

To form the coumarin triflate reagent **1**, a solution of Tf_2O (27.6 µl, 164 µmol, 1.0 equiv., 1:10 dilution in DCM) was added to an ice-cold solution of 7-diethylamino 4-hydroxymethyl coumarin (42 mg, 170 µmol, 1.04 equiv.) and DIEA (100 µl, 0.575 mmol) in 2 ml dry DCM under inert conditions in an ice bath. After 2 minutes the resulting activated coumarin solution was transferred into a precooled flask with a solution of oleic acid in 2 ml chloroform (46 mg, 163 µmol, 1.0 equiv.). After 3 hours the reaction was quenched by adding 1 ml MeOH, followed by the removal of all volatiles under reduced pressure. The crude product was purified by flash column chromatography (2 times, 1-3 % MeOH in DCM) to yield 47 mg of a yellow solid (92 µmol, 56 %).

HR-MS (ESI positive) m/z found: calculated for $C_{32}H_{49}NO_4$: 511.3662; found: 512.371 $[M+H]^+$

^1H NMR (400 MHz, $CDCl_3$) δ = 7.29 (d, J = 9.0 Hz, 1H), 6.59 (dd, J = 9.0, 2.6 Hz, 1H), 6.52 (d, J = 2.5 Hz, 1H), 6.13 (s, 1H), 5.40 – 5.29 (m, 2H), 5.21 (s, 2H), 3.41 (q, J = 7.1 Hz, 4H), 2.43 (t, J = 7.6 Hz, 2H), 2.05 – 1.95 (m, 4H), 1.74 – 1.64 (m, 2H), 1.38 – 1.23 (m, 20H), 1.20 (t, J = 7.1 Hz, 6H), 0.87 (t, J = 6.7 Hz, 3H) ppm.

^{13}C NMR (101 MHz, DMSO) δ = 172.91, 161.07, 156.29, 151.08, 150.95, 130.12, 130.05, 125.95, 109.21, 105.79, 105.73, 97.32, 61.54, 44.47, 33.74, 31.74, 29.55, 29.47, 29.29, 29.14, 29.05, 28.94, 28.88, 28.86, 27.03, 27.00, 24.85, 22.55, 14.39, 12.77 ppm.

9.7. Caged PAF, cg PAF, 10

2-((((R)-2-acetoxy-3-(hexadecyloxy)propoxy)((7-(diethylamino)-2-oxo-2H-chromen-4-yl)methoxy)phosphoryl)oxy)-N,N,N-trimethylethan-1-aminium.

To form the coumarin triflate reagent **1**, a solution of Tf_2O (24 µl, 142 µmol, 1.13 equiv., 1:10 dilution in DCM) was added to an ice-cold solution of 7-diethylamino 4-hydroxymethyl coumarin (35 mg, 142 µmol, 1.13 equiv.) and DIEA (100 µl, 0.575 mmol) in 1.5 ml dry DCM under inert conditions in an ice bath. After 2 minutes the resulting activated coumarin solution was transferred into a precooled flask with a solution of PAF in 2 ml dry chloroform (66 mg, 126 µmol, 1.0 equiv.). After 60 minutes a freshly prepared solution of the activated coumarin (0.6 equiv.) was added and the reaction mixture was slowly allowed to reach room temperature. After 3 hours the reaction was quenched by adding 1 ml MeOH, followed by the removal of all volatiles under reduced pressure. The crude product was dissolved in MeOH and purified by preparative gradient RP-HPLC using a Knauer Azura system with a NUCLEODUR® C18 Pyramid column. With a constant flowrate of 15 ml/min, 100 % solvent A (500 ml water, 250 ml MeOH, 250 ml 2-propanol with 0.01 % TFA) was kept for 3 minutes. Using a linear gradient reaching 100 % solvent B (2-propanol with 0.01 %) after 23 min, holding 100 % B until 29 min, the pure product elutes from 14.5 - 16 min. 72 mg of a yellow solid were obtained (96 µmol, 76 %).

HR-MS (ESI positive) m/z found: calculated for $C_{40}H_{70}N_2O_9P^+$: 753.4813; found: 753.485 $[M]^+$

^{1}H NMR (400 MHz, MeOD) δ = 7.47 (2xd, J = 9.1Hz, 1H), 6.76 (dd, J = 9.1, 2.6 Hz, 1H), 6.58 (d, J = 2.5 Hz, 1H), 6.16 (2xs, 1H), 5.42 – 5.33 (m, 2H), 5.27 – 5.11 (m, 1H), 4.67 – 4.58 (m, 2H), 4.44 – 4.24 (m, 2H), 3.82 – 3.74 (m, 2H), 3.63 – 3.35 (m, 8H), 3.23 (s, 9H), 2.06 (d, J = 2.1 Hz, 3H), 1.57 – 1.48 (m, 2H), 1.35-1.15 (m, 32H), 0.90 (t, J = 6.8 Hz, 3H) ppm, two diastereomers present.

^{13}C carbon resonances that exhibit coupling patterns due to ^{31}P-^{13}C couplings or due to the presence of two diastereomers, as well as overlapping peaks in the aliphatic regions are marked as multiplets (m) in the peak list and given as a range.

^{13}C NMR (101 MHz, MeOD) δ = 171.97, 164.00, 157.65, 152.63, 151.82-151.76 (m), 126.10, 110.53, 106.62, 106.51-106.48 (m), 98.45, 72.76, 72.25-72.16 (m), 69.29, 68.73- 68.58 (m), 66.86 (m), 66.75-66.70 (m), 63.03-62.99 (m), 54.60-54.53 (m), 45.69, 33.07, 30.78-30.73 (m), 30.64, 30.54, 30.47, 27.17, 23.73, 20.94-20.92 (m), 14.43, 12.73 ppm.

^{31}P NMR (162 MHz, DMSO) δ = -1.70, -1.73 ppm.

9.8. Caged miltefosine, cg MF, 11

2-((((7-(diethylamino)-2-oxo-2H-chromen-4-yl)methoxy)(pentadecyloxy)phosphoryl)oxy)-N,N,N-trimethylethan-1-aminium.

To form the coumarin triflate reagent **1**, a solution of Tf_2O (24 µl, 142 µmol, 1.13 equiv., 1:10 dilution in DCM) was added to an ice-cold solution of 7-diethylamino 4-hydroxymethyl coumarin (35 mg, 142 µmol, 1.13 equiv.) and DIEA (100 µl, 0.575 mmol) in 1.5 ml dry DCM under inert conditions in an ice bath. After 2 minutes the resulting activated coumarin solution was transferred into a precooled flask with a solution of miltefosin in 5 ml dry chloroform (51.3 mg, 126 µmol, 1.0 equiv.). After 60 minutes a freshly prepared solution of the activated coumarin (0.6 equiv.) was added and the reaction mixture was allowed to slowly reach room temperature. After 3 hours the reaction was quenched by adding 1 ml MeOH followed by the removal of all volatiles under reduced pressure. The crude product was dissolved in MeOH and purified by preparative gradient RP-HPLC using a Knauer Azura system with a NUCLEODUR® C18 Pyramid column. A constant flowrate of 15 ml/min, 100 % solvent A (500 ml water, 250 ml MeOH, 250 ml 2-propanol with 0.01% TFA) was kept for 3 minutes. Using a linear gradient reaching 100 % solvent B (2-propanol with 0.01 % TFA) after 23 min, and holding 100 % B until 29 min, the pure product eluted from 14.5 - 16 min. 50 mg of a yellow solid were obtained (80.1 µmol, 63.5 %).

HR-MS (ESI positive) m/z found: calculated for $C_{35}H_{62}N_2O_6P^+$: 637.434; found: 637.435 $[M]^+$

^1H NMR (400 MHz, MeOD) δ = 7.48 (d, J = 9.0 Hz, 1H), 6.74 (dd, J = 9.1, 2.6 Hz, 1H), 6.55 (d, J = 2.5 Hz, 1H), 6.15 (s, 1H), 5.35 (2xs, 2H), 4.61 (m, 2H), 4.18 (m, 2H), 3.82 – 3.75 (m, 2H), 3.48 (q, J = 7.1 Hz, 4H), 3.24 (s, 9H), 1.69 (m, 2H), 1.41 – 1.17 (m, 32H), 0.89 (t, J = 6.8 Hz, 3H) ppm, two diastereomers present.

^{13}C carbon resonances that exhibit coupling patterns due to ^{31}P-^{13}C couplings or duplications due to the presence of two diastereomers, as well as overlapping peaks in the aliphatic regions are marked as multiplets (m) in the peak list and given as a range.

^{13}C NMR (101 MHz, MeOD) δ = 163.98, 157.62, 152.56, 151.94-151.87 (m), 126.18, 110.52, 106.72, 106.65, 98.43, 70.69-70.63 (m), 66.89-66.81 (m), 66.59-66.54 (m), 62.77-62.72 (m), 54.60-54.52 (m), 45.70, 33.07, 31.29, 31.23, 30.78-30.75 (m), 30.67, 30.61, 30.47, 30.20, 26.52, 23.73, 14.44, 12.74 ppm.

^{31}P NMR (162 MHz, MeOD) δ = -1.86 ppm.

9.9. Caged edelfosine, cg EF, 12

2-((((7-(diethylamino)-2-oxo-2H-chromen-4-yl)methoxy)((R)-2-methoxy-3(octadecyloxy) propoxy)phosphoryl)oxy)-N,N,N-trimethylethan-1-aminium.

To form the coumarin triflate reagent **1**, a solution of Tf_2O (12 µl, 69 µmol, 1.03 equiv., 1:10 dilution in DCM) was added to an ice-cold solution of 7-diethylamino 4-hydroxymethyl coumarin (17 mg, 69 µmol, 1.03 equiv.) and DIEA (100 µl, 0.575 mmol) in 1.5 ml dry DCM under inert conditions in an ice bath. After 2 minutes the resulting activated coumarin solution was transferred into a precooled flask with a solution of edelfosin in 5 ml dry chloroform (35 mg, 67 µmol, 1.0 equiv.). After 60 minutes a freshly prepared solution of the activated coumarin (0.6 equiv.) was added and the reaction mixture was allowed to slowly reach room temperature. After 3 hours the reaction was quenched by adding 1 ml MeOH followed by the removal of all volatiles under reduced pressure. The crude product was dissolved in MeOH and purified by preparative gradient RP-HPLC using a Knauer Azura system with a NUCLEODUR® C18 Pyramid column. A constant flowrate of 15 ml/min, 100 % solvent A (500 ml water, 250 ml MeOH, 250 ml 2-propanol with 0.01 % TFA) was kept for 3 minutes. Using a linear gradient reaching 50 % solvent B (2-propanol with 0.01 % TFA) after 10 min and 100 % B after 26 min, holding 100 % B until 29 min, the pure product eluted from 12-14 min. 18 mg of a yellow solid were obtained (24 µmol, 36 %).

HR-MS (ESI positive) m/z found: calculated for $C_{41}H_{74}N_2O_8P^+$: 753.5177; found: 753.5152 $[M]^+$

^{1}H NMR (400 MHz, MeOD) δ = 7.47 (d, J = 9.1 Hz, 1H), 6.76 (dd, J = 9.1, 2.6 Hz, 1H), 6.57 (d, J = 2.5 Hz, 1H), 6.17 (s, 1H), 5.38 (m_c, 2H), 4.68 – 4.58 (m, 2H), 4.44 – 4.12 (m, 2H), 3.82 – 3.75 (m, 2H), 3.64 – 3.56 (m, 1H), 3.55 – 3.39 (m, 11H), 3.24 (s, 9H), 1.56 – 1.46 (m, 2H), 1.33 – 1.17 (m, 36H), 0.90 (t, J = 6.8 Hz, 3H) ppm, two diastereomers present.

^{13}C carbon resonances that exhibit coupling patterns due to ^{31}P-^{13}C couplings or due to the presence of two diastereomers, as well as overlapping peaks in the aliphatic regions are marked as multiplets (m) in the peak list and given as a range.

^{13}C NMR (101 MHz, MeOD) δ = 164.05-164.02 (m), 157.63, 152.58, 151.96-151.90 (m), 126.08, 110.52, 106.67, 106.50-106.45 (m), 98.46, 79.80- 79.68 (m), 72.77-72.74 (m), 69.59-69.49 (m), 69.34-69.18 (m), 66.86 (m), 66.62- 66.49 (m), 62.96-62.84 (m), 58.16-58.15 (m), 54.61-54.53 (m), 45.70, 33.07, 30.77- 30.71 (m), 30.57, 30.47, 27.22, 23.73, 14.44, 12.73 ppm.

^{31}P NMR (162 MHz, MeOD) δ = -1.84 ppm.

9.10. Caged prostaglandin E_2, cg PGE_2, 13

(7-(diethylamino)-2-oxo-2H-chromen-4-yl)methyl (Z)-7-((1R,2R,3R)-3-hydroxy-2-((S,E)-3-hydroxyoct-1-en-1-yl)-5-oxocyclopentyl)hept-5-enoate.

To form the coumarin triflate reagent **1**, a solution of Tf_2O (27.6 µl, 164 µmol, 1.16 equiv., 1:10 dilution in DCM) was added to an ice-cold solution of 7-diethylamino 4-hydroxymethyl coumarin (42 mg, 170 µmol, 1.2 equiv.) and DIEA (100 µl, 0.59 mmol) in 1.5 ml dry DCM under inert conditions in an ice bath. After 2 minutes the resulting activated coumarin solution was transferred into a precooled flask with a solution of PGE_2 in 1.5 ml chloroform (50 mg, 142 µmol, 1.0 equiv.). After 3 hours the reaction was quenched by adding 1 ml MeOH followed by the removal of all volatiles under reduced pressure. The crude product was purified by flash column chromatography (1. 1-5 % MeOH in DCM; 2. 5 % MeOH in DCM) to yield 60 mg of a yellow solid (103 µmol, 73 %).

HR-MS (ESI positive) m/z found: calculated for $C_{34}H_{47}NO_7$: 581.3353; found: 582.3453 $[M+H]^+$

^1H NMR (400 MHz, $CDCl_3$) δ = 7.22 (d, J = 9.0 Hz, 1H), 6.53 (dd, J = 9.0, 2.6 Hz, 1H), 6.44 (d, J = 2.5 Hz, 1H), 6.05 (s, 1H), 5.63 – 5.42 (m, 2H), 5.38 – 5.22 (m, 2H), 5.16 (d, J = 1.4 Hz, 2H), 4.06 – 3.92 (m, 2H), 3.35 (q, J = 7.1 Hz, 4H), 2.72 – 2.60 (m, 1H), 2.45 – 2.20 (m, 5H), 2.14 (dd, J = 18.5, 9.8 Hz, 1H), 2.08 – 1.92 (m, 3H), 1.75 – 1.62 (m, 2H), 1.57 – 1.34 (m, 2H), 1.31 – 1.09 (m, 12H), 0.80 (t, J = 6.9 Hz, 3H) ppm.

^{13}C NMR (101 MHz, $CDCl_3$) δ = 214.24, 172.82, 162.19, 156.20, 150.70, 149.89, 137.02, 131.42, 130.49, 126.93, 124.42, 108.90, 106.09, 97.88, 77.24, 72.95, 71.98, 61.18, 54.52, 53.76, 46.07, 44.83, 37.18, 33.45, 31.73, 26.57, 25.20, 25.11, 24.59, 22.64, 14.04, 12.42 ppm.

9.11. Caged 2-hydroxy oleic acid, cg OHOA, 14

(7-(diethylamino)-2-oxo-2H-chromen-4-yl)methyl (Z)-2-hydroxyoctadec-9-enoate.

125 mg (390 µmol, 1.0 equiv.) of the sodium salt of 2-hydroxy oleic acid were first treated with 100 ml 0.4 % HCL and subsequently extracted with 50 ml DCM and 50 ml ethyl acetate. The combined organic layers were washed with 30 ml of water each, combined and dried over Na_2SO_4 and the solvent removed under reduced pressure. The resulting free acid was dissolved in 1.5 ml dry chloroform. Then, a solution of Tf_2O (65 µl, 386 µmol, 1.0 equiv., 1:10 dilution in DCM) was added to an ice-cold solution of 7-diethylamino 4-hydroxymethyl coumarin (100 mg, 404 µmol, 1.04 equiv.) and DIEA (300 µl, 1.77 mmol) in 3 ml dry DCM under inert conditions in an ice bath to form the coumarin triflate reagent **1**. After 2 minutes the activated coumarin solution was transferred into the precooled flask charged with the solution of 2-OHOA in 1.5 ml chloroform. After 1.75 hours the reaction was quenched by adding 1 ml MeOH followed by the removal of all volatiles under reduced pressure. The crude product was purified by flash column chromatography (2.5 % MeOH in DCM) to yield 100 mg of an orange solid (190 µmol, 49 %).

HR-MS (ESI positive) m/z found: calculated for $C_{32}H_{49}NO_5$: 527.3611; found: 528.37153 $[M+H]^+$

^1H NMR (400 MHz, MeOD) δ = 7.41 (d, J = 9.0 Hz, 1H), 6.68 (dd, J = 9.1, 2.6 Hz, 1H), 6.48 (d, J = 2.5 Hz, 1H), 6.04 (s, 1H), 5.39 – 5.23 (m, 4H), 4.31-4.26 (m, 1H), 3.44 (q, J = 7.1 Hz, 4H), 2.06-1.92 (m, 4H), 1.87 – 1.64 (m, 2H), 1.47 – 1.15 (m, 26H), 0.87 (t, J = 6.8 Hz, 3H) ppm.

^{13}C NMR (101 MHz, MeOD) δ = 173.82, 162.66, 156.13, 151.03, 150.82, 129.52, 129.36, 124.84, 108.98, 105.76, 105.28, 96.94, 70.33, 61.44, 44.27, 33.99, 31.70, 29.49, 29.38, 29.26, 29.10, 29.00, 28.94, 28.81, 26.79, 26.76, 24.67, 22.38, 13.15, 11.48 ppm.

9.12. Caged N-acetyl neuraminic acid, cg NANA, 15

(7-(diethylamino)-2-oxo-2H-chromen-4-yl)methyl (2R,4S,5R,6R)-5-acetamido-2,4-di hydroxy-6-((1R,2R)-1,2,3-trihydroxypropyl)tetrahydro-2H-pyran-2-carboxylate

To form the coumarin triflate reagent **1**, a solution of Tf_2O (24 µl, 142 µmol, 1.07 equiv., 1:10 dilution in DCM) was added to an ice-cold solution of 7-diethylamino 4-hydroxymethyl coumarin (35 mg, 142 µmol, 1.07 equiv.) and DIEA (200 µl, 1.15 mmol) in 1.5 ml dry DCM under inert conditions in an ice bath. After 2 minutes the resulting activated coumarin solution was transferred into a precooled flask with a solution of N-acetyl-neuraminic acid in 3 ml dry DMF (41 mg, 133 µmol, 1.0 equiv.). After 60 minutes a freshly prepared solution of the activated coumarin (0.6 equiv.) was added and the reaction mixture was slowly allowed to reach room temperature. After 3 hours the reaction was quenched by adding 1 ml MeOH followed by the removal of all volatiles under reduced pressure. The crude product was dissolved in MeOH and purified by preparative gradient RP-HPLC using a Knauer Azura system with a NUCLEODUR® C18 Pyramid column. With a constant flowrate of 20 ml/min, 100 % solvent A (10% MeOH in water with 0.01 % TFA) was kept for 3 minutes. Using a linear gradient reaching 50 % solvent B (90 % MeOH in water with 0.01 % TFA) after 8 min and 100 % B after 26 min, holding 100 % B until 29 min, the pure product eluted after 15 min. 41 mg of a yellow solid were obtained (76 µmol, 57 %).

HR-MS (ESI positive) m/z found: calculated for $C_{25}H_{34}NO_{11}$: 538.2163; found: 539.222 $[M+H]^+$

^{1}H NMR (400 MHz, MeOD) δ = 7.50 (d, J = 9.1 Hz, 1H), 6.76 (dd, J = 9.1, 2.6 Hz, 1H), 6.55 (d, J = 2.6 Hz, 1H), 6.16 (s, 1H), 5.46 – 5.35 (m, 2H), 4.13 – 4.00 (m, 2H), 3.90 – 3.84 (m, 1H), 3.84 – 3.78 (m, 1H), 3.78 – 3.72 (m, 1H), 3.66 (dd, J = 11.2, 5.2 Hz, 1H), 3.57 – 3.44 (m, 5H), 2.30 (dd, J = 12.8, 5.0 Hz, 1H), 2.06 – 1.93 (m, 4H), 1.21 (t, J = 7.1 Hz, 6H) ppm.

^{13}C NMR (101 MHz, MeOD) δ = 175.16, 170.42, 164.24, 157.55, 152.53, 152.20, 126.31, 110.54, 107.10, 106.41, 98.26, 72.36, 71.60, 70.10, 67.78, 64.78, 63.58, 54.36, 45.62, 40.72, 22.63, 12.73 ppm.

1 Nadler, A. *et al.* Exclusive photorelease of signalling lipids at the plasma membrane. *Nat Commun* **6**, 10056, doi:10.1038/ncomms10056 (2015).
2 Wagner, N., Stephan, M., Höglinger, D. & Nadler, A. A Click Cage: Organelle-Specific Uncaging of Lipid Messengers. *Angew Chem Int Edit* **57**, 13339-13343, doi:doi:10.1002/anie.201807497 (2018).
3 Stein, F., Kress, M., Reither, S., Piljić, A. & Schultz, C. FluoQ: A Tool for Rapid Analysis of Multiparameter Fluorescence Imaging Data Applied to Oscillatory Events. *ACS Chem Biol* **8**, 1862-1868, doi:10.1021/cb4003442 (2013).
4 Weinrich, T., Gränz, M., Grünewald, C., Prisner, T. F. & Göbel, M. W. Synthesis of a Cytidine Phosphoramidite with Protected Nitroxide Spin Label for EPR Experiments with RNA. *Eur J Org Chem* **2017**, 491-496, doi:10.1002/ejoc.201601174 (2017).
5 Wong, P. T. *et al.* Control of an Unusual Photo-Claisen Rearrangement in Coumarin Caged Tamoxifen through an Extended Spacer. *ACS Chem Biol* **12**, 1001-1010, doi:10.1021/acschembio.6b00999 (2017).
6 Ito, K. & Maruyama, J. Studies on Stable Diazoalkanes as Potential Fluorogenic Reagents. I. 7-Substituted 4-Diazomethylcoumarins. *Chem Pharm Bull* **31**, 3014-3023 (1983).

10.NMR spectra of compounds

Shown are the ^{1}H, ^{13}C and if applicable the ^{31}P spectra of compounds **5** – **15**.

(**5**, cg POPC)

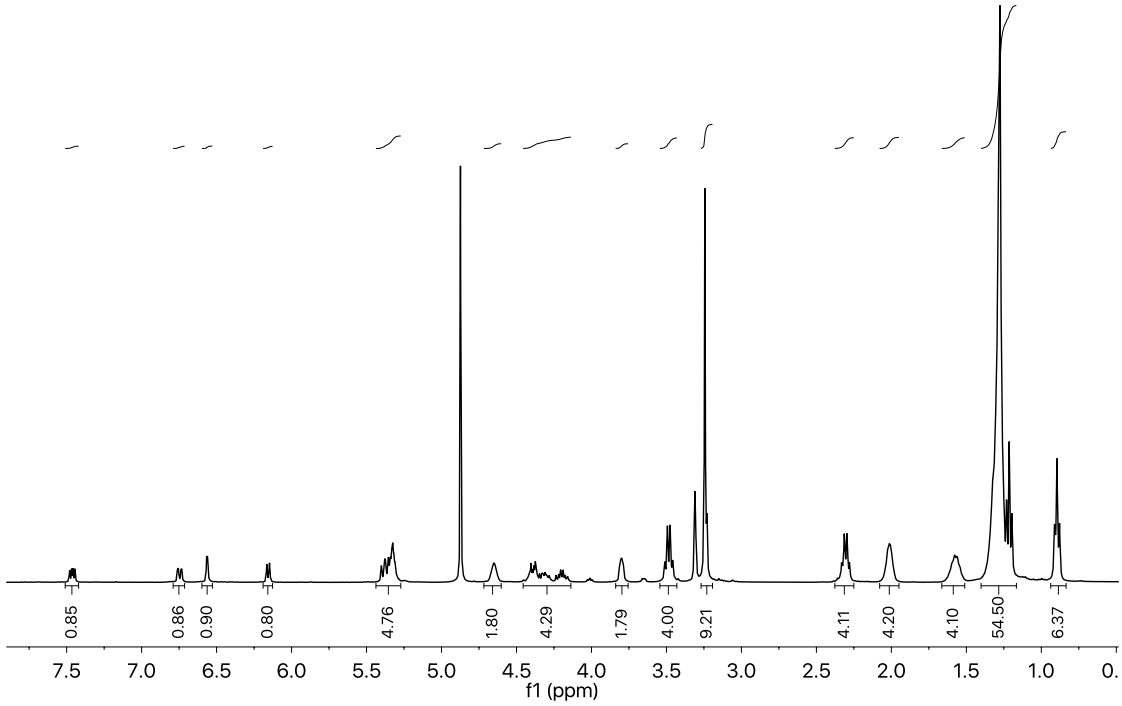
0.85
0.86
0.90
0.80
4.76
1.80
4.29
1.79
4.00
9.21
4.11
4.20
4.10
54.50
6.37
7.5 7.0 6.5 6.0 5.5 5.0 4.5 4.0 3.5 3.0 2.5 2.0 1.5 1.0 0.
f1 (ppm)

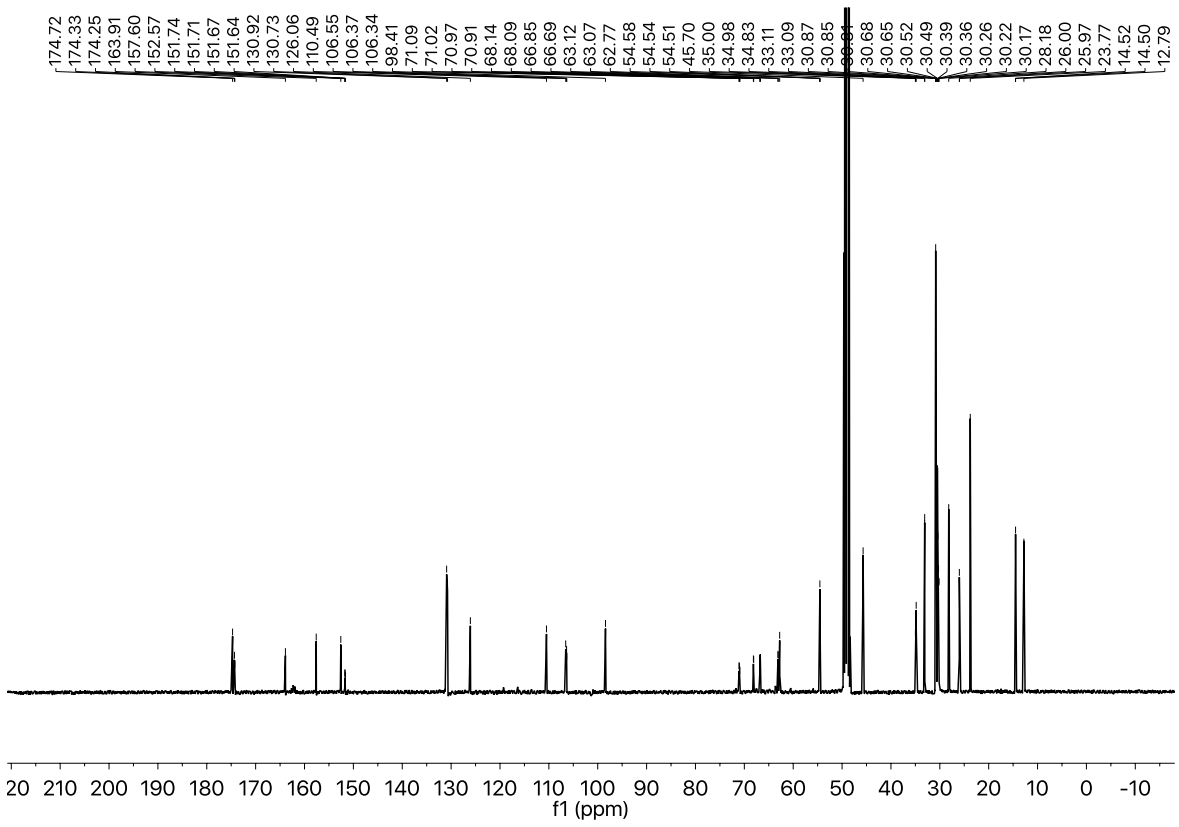
174.72
174.33
174.25
163.91
157.60
152.57
151.74
151.71
151.67
151.64
130.92
130.73
126.06
110.49
106.55
106.37
106.34
98.41
71.09
71.02
70.97
70.91
68.14
68.09
66.85
66.69
63.12
63.07
62.77
54.58
54.54
54.51
45.70
35.00
34.98
34.83
33.11
33.09
30.87
30.85
30.68
30.65
30.52
30.49
30.39
30.36
30.26
30.22
30.17
28.18
26.00
25.97
23.77
14.52
14.50
12.79
20 210 200 190 180 170 160 150 140 130 120 110 100 90 80 70 60 50 40 30 20 10 0 -10
f1 (ppm)

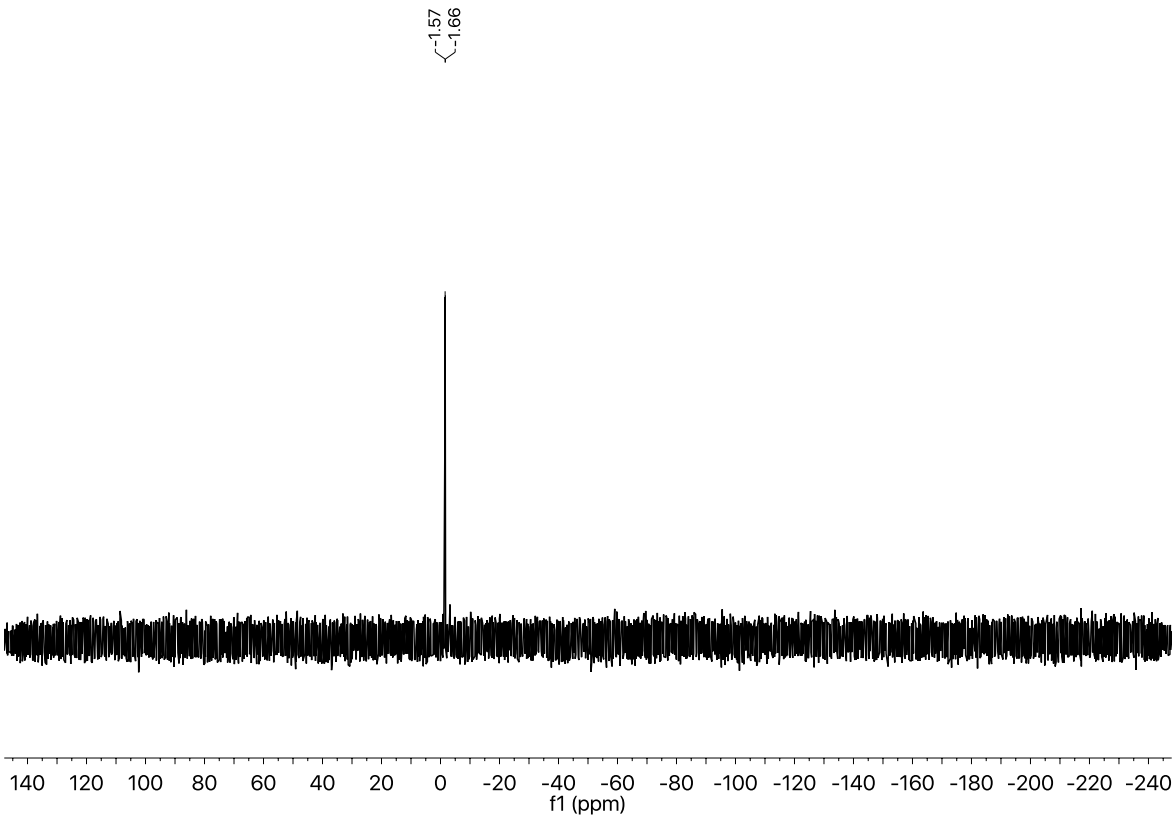
-1.57
-1.66
140 120 100 80 60 40 20 0 -20 -40 -60 -80 -100 -120 -140 -160 -180 -200 -220 -240
f1 (ppm)

(**6**, cg LPA)

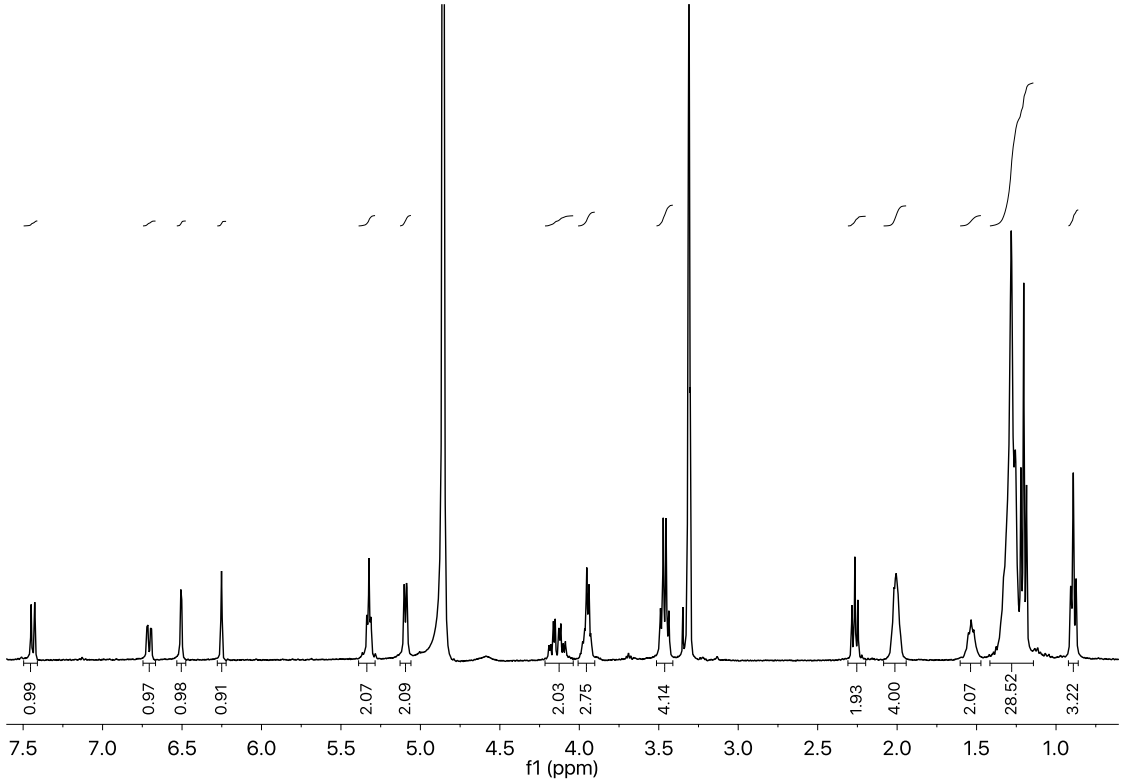
0.99
0.97
0.98
0.91
2.07
2.09
2.03
2.75
4.14
1.93
4.00
2.07
28.52
3.22
7.5
7.0
6.5
6.0
5.5
5.0
4.5
4.0
3.5
3.0
2.5
2.0
1.5
1.0
f1 (ppm)

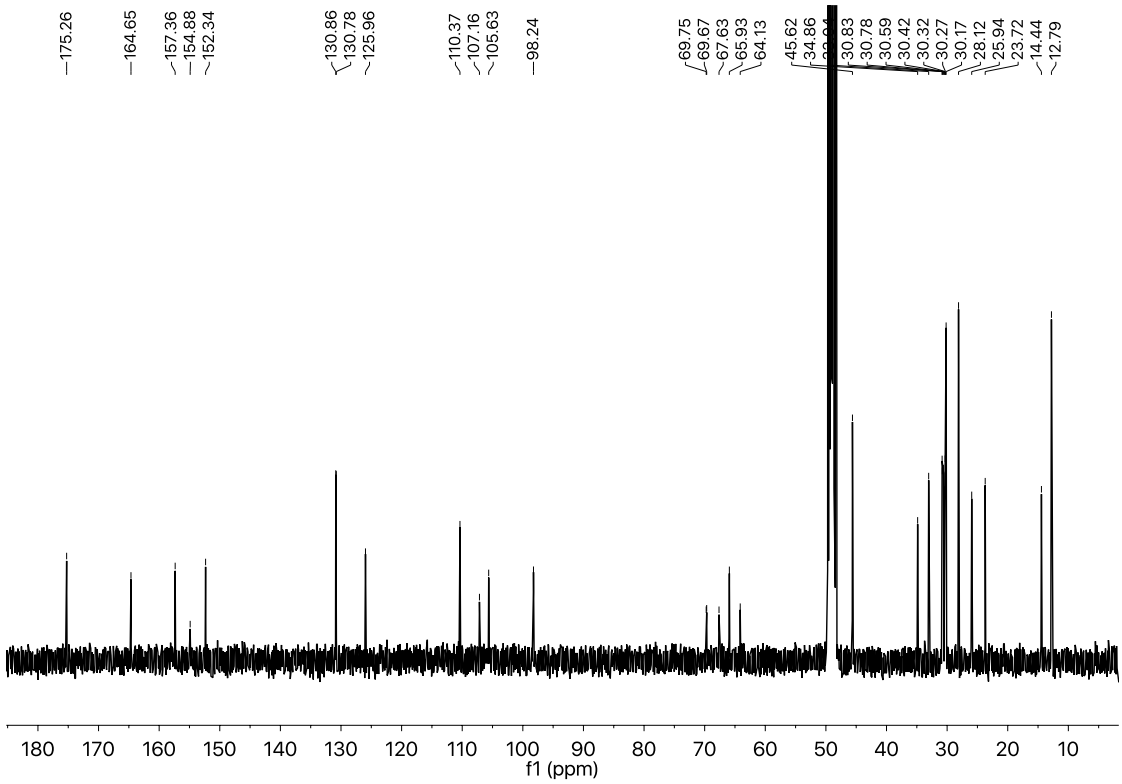
175.26
164.65
157.36
154.88
152.34
130.86
130.78
125.96
110.37
107.16
105.63
98.24
69.75
69.67
67.63
65.93
64.13
45.62
34.86
30.83
30.78
30.59
30.42
30.32
30.27
30.17
28.12
25.94
23.72
14.44
12.79
180
170
160
150
140
130
120
110
100
90
80
70
60
50
40
30
20
10
f1 (ppm)

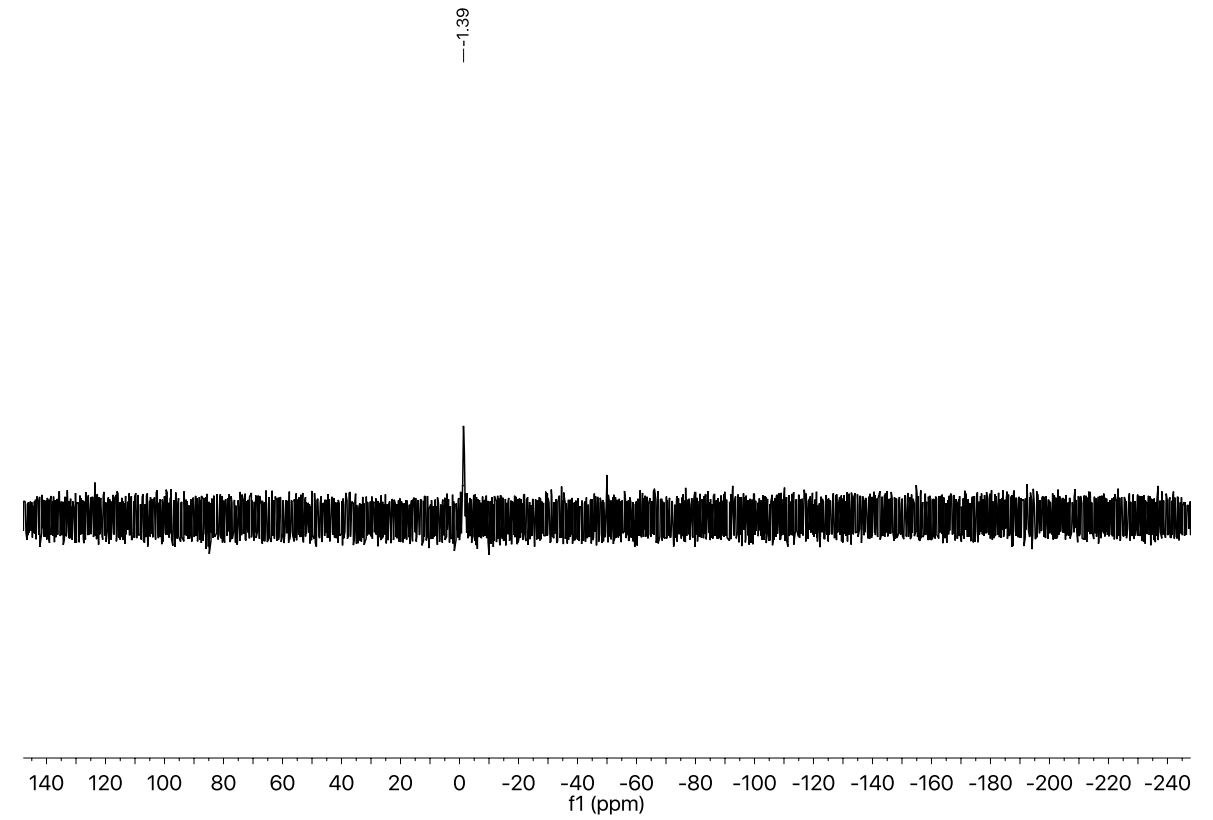
-1.39
140 120 100 80 60 40 20 0 -20 -40 -60 -80 -100 -120 -140 -160 -180 -200 -220 -240
f1 (ppm)

(**7**, DOPA)

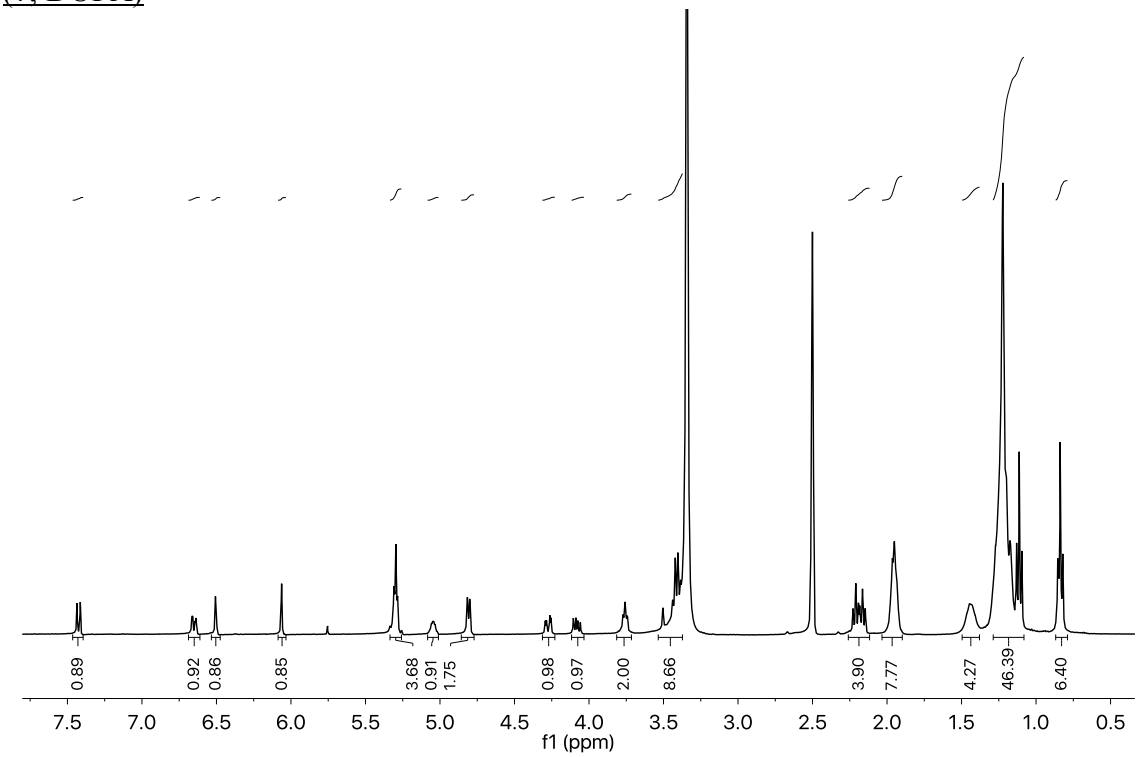
0.89
0.92
0.86
0.85
3.68
0.91
1.75
0.98
0.97
2.00
8.66
3.90
7.77
4.27
46.39
6.40
7.5 7.0 6.5 6.0 5.5 5.0 4.5 4.0 3.5 3.0 2.5 2.0 1.5 1.0 0.5
f1 (ppm)

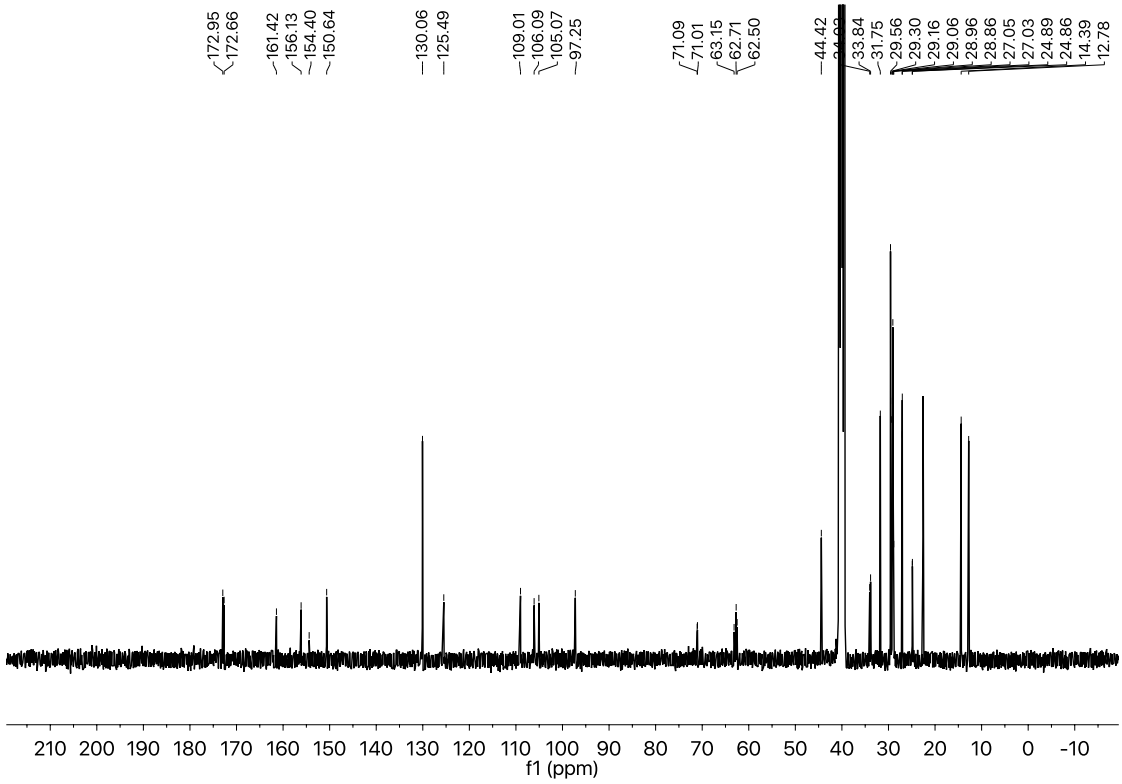
172.95
172.66
161.42
156.13
154.40
150.64
130.06
125.49
109.01
106.09
105.07
97.25
71.09
71.01
63.15
62.71
62.50
44.42
33.84
31.75
29.56
29.30
29.16
29.06
28.96
28.86
27.05
27.03
24.89
24.86
14.39
12.78
210 200 190 180 170 160 150 140 130 120 110 100 90 80 70 60 50 40 30 20 10 0 -10
f1 (ppm)

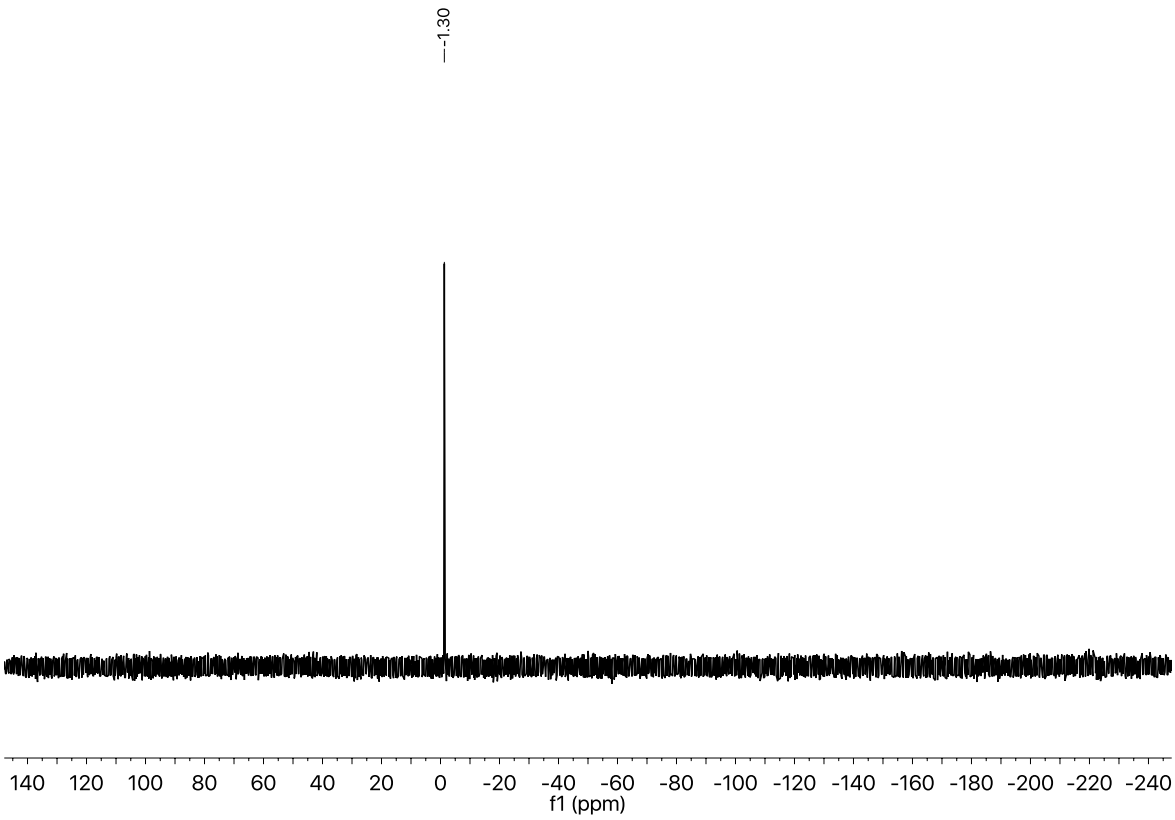
-1.30
140 120 100 80 60 40 20 0 -20 -40 -60 -80 -100 -120 -140 -160 -180 -200 -220 -240
f1 (ppm)

(**8**, cg arachidonic acid)

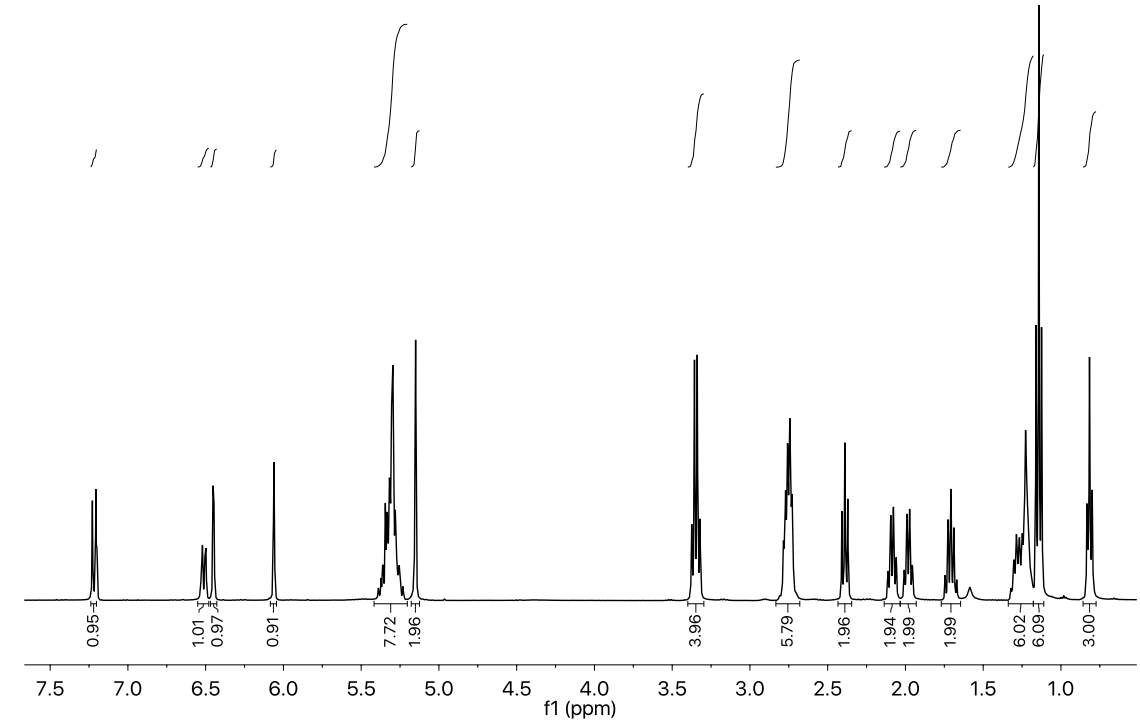

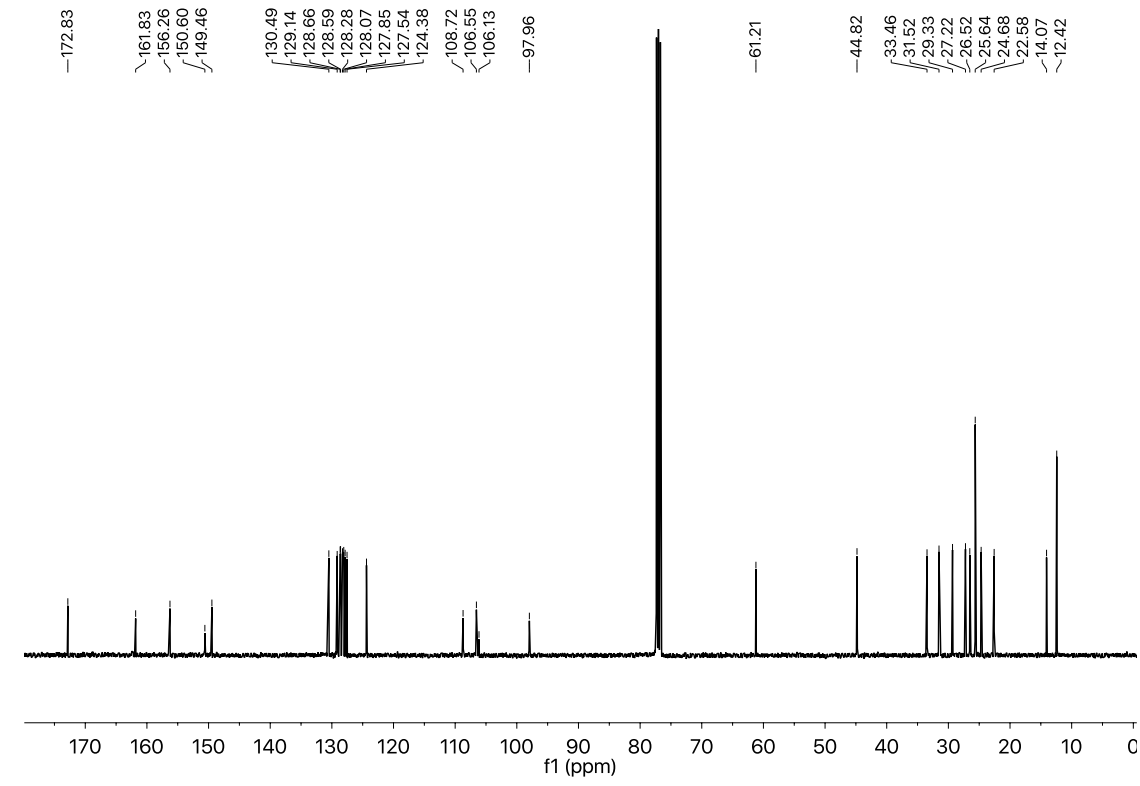

(**9**, cg oleic acid)

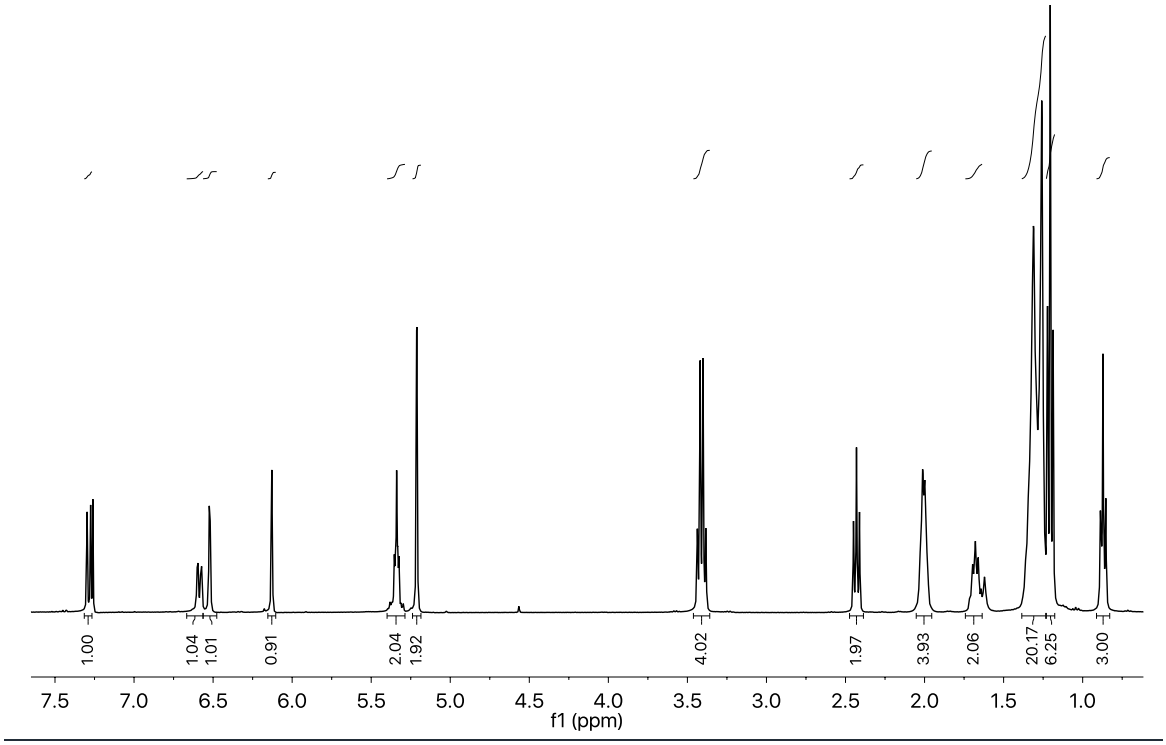

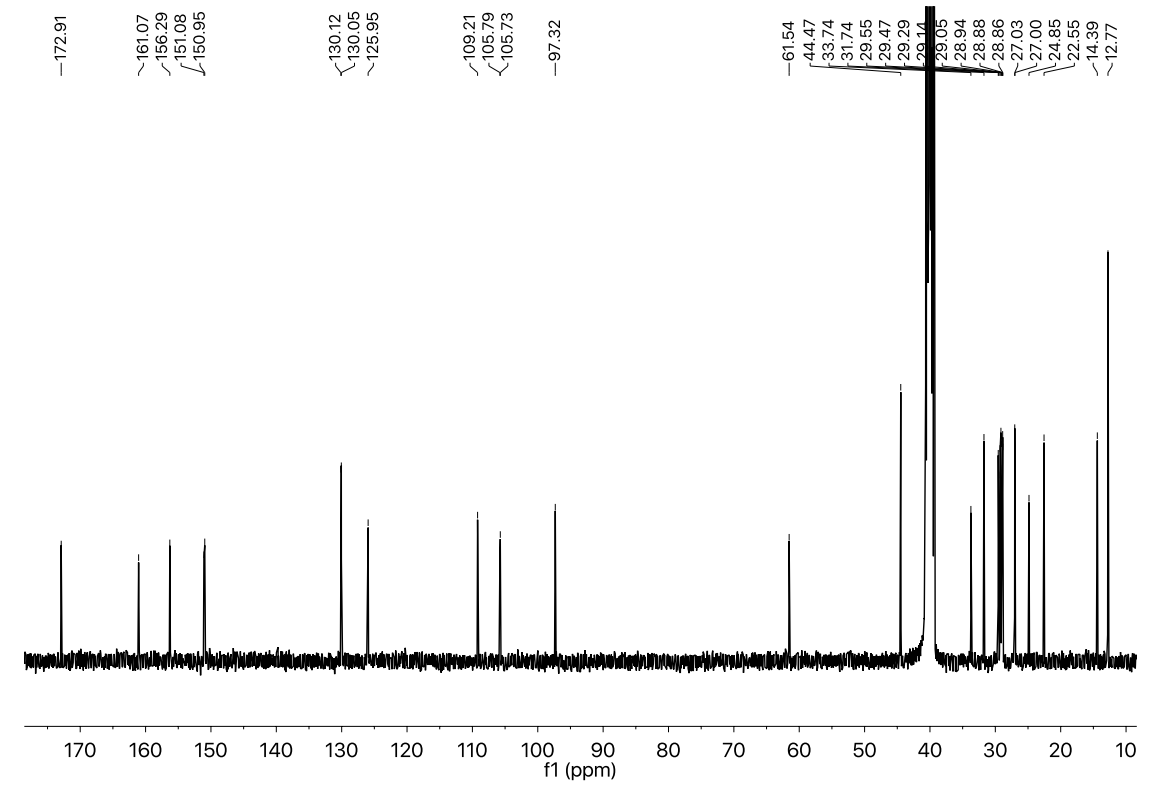

(**10**, cg PAF)

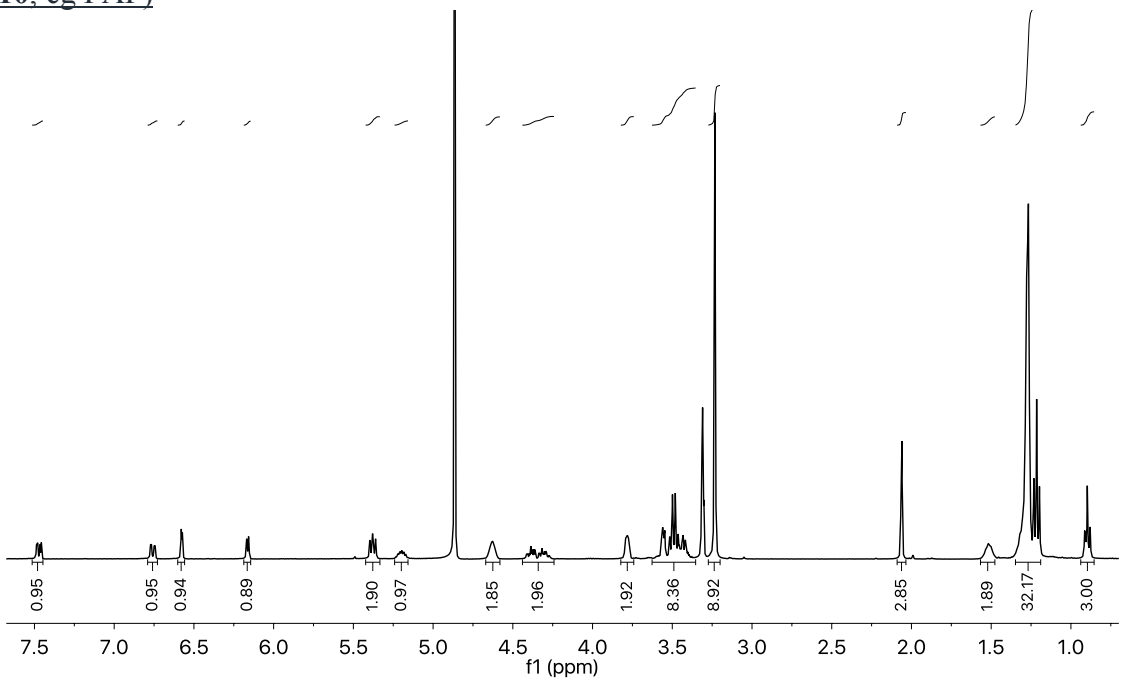
0.95
0.95
0.94
0.89
1.90
0.97
1.85
1.96
1.92
8.36
8.92
2.85
1.89
32.17
3.00
7.5 7.0 6.5 6.0 5.5 5.0 4.5 4.0 3.5 3.0 2.5 2.0 1.5 1.0
f1 (ppm)

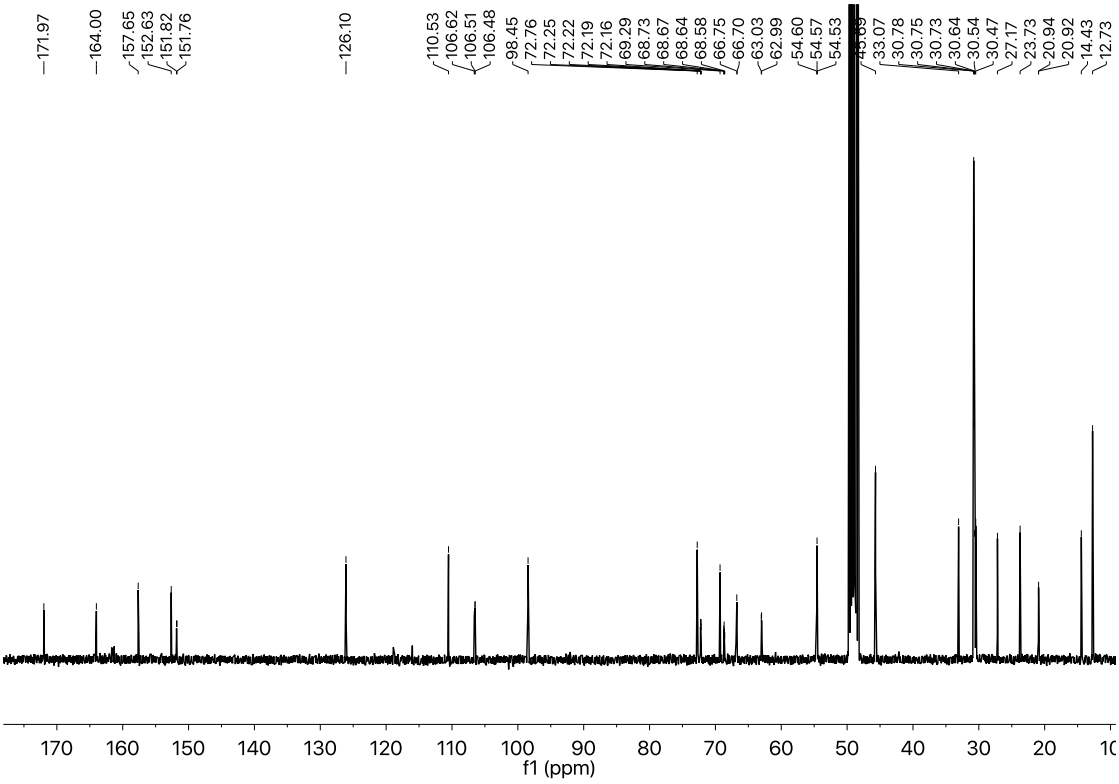
171.97
164.00
157.65
152.63
151.82
151.76
126.10
110.53
106.62
106.51
106.48
98.45
72.76
72.25
72.22
72.19
72.16
69.29
68.73
68.67
68.64
68.58
66.75
66.70
63.03
62.99
54.60
54.57
54.53
33.07
30.78
30.75
30.73
30.64
30.54
30.47
27.17
23.73
20.94
20.92
14.43
12.73
170 160 150 140 130 120 110 100 90 80 70 60 50 40 30 20
f1 (ppm)

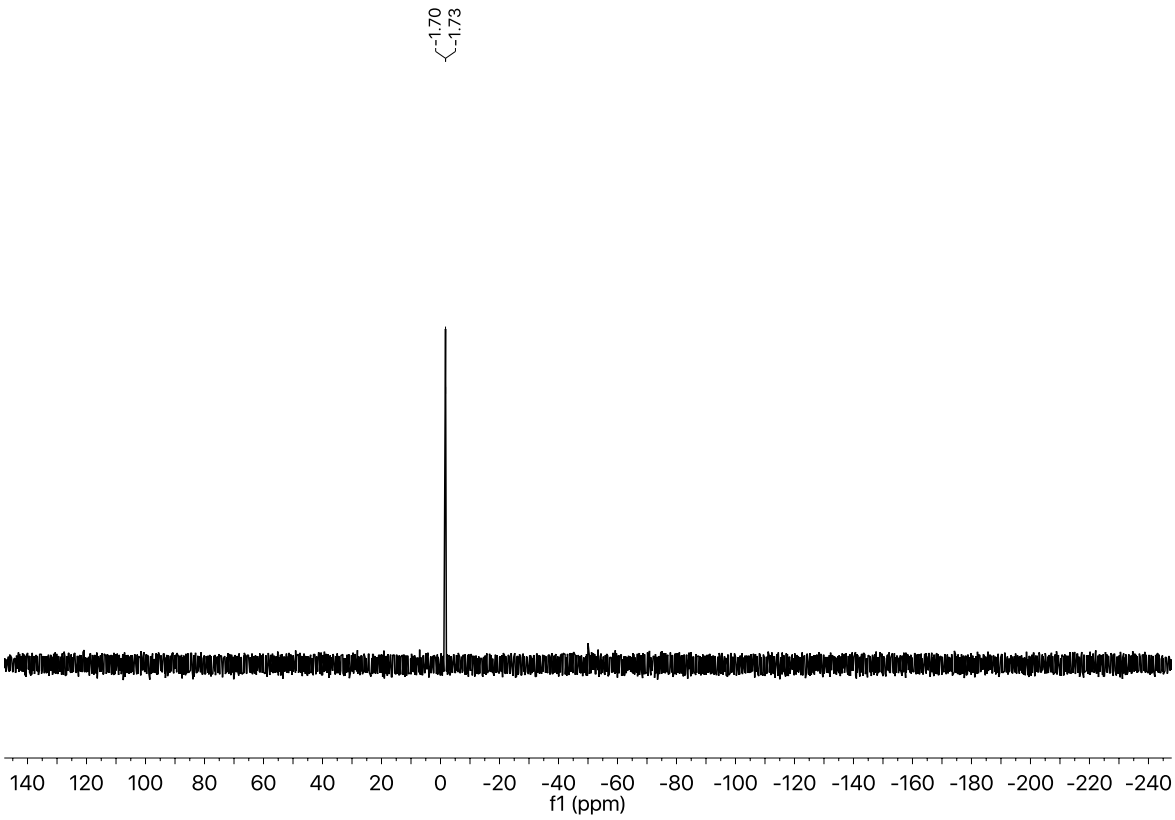
-1.70
-1.73
140 120 100 80 60 40 20 0 -20 -40 -60 -80 -100 -120 -140 -160 -180 -200 -220 -240
f1 (ppm)

(**11**, cg miltefosin)

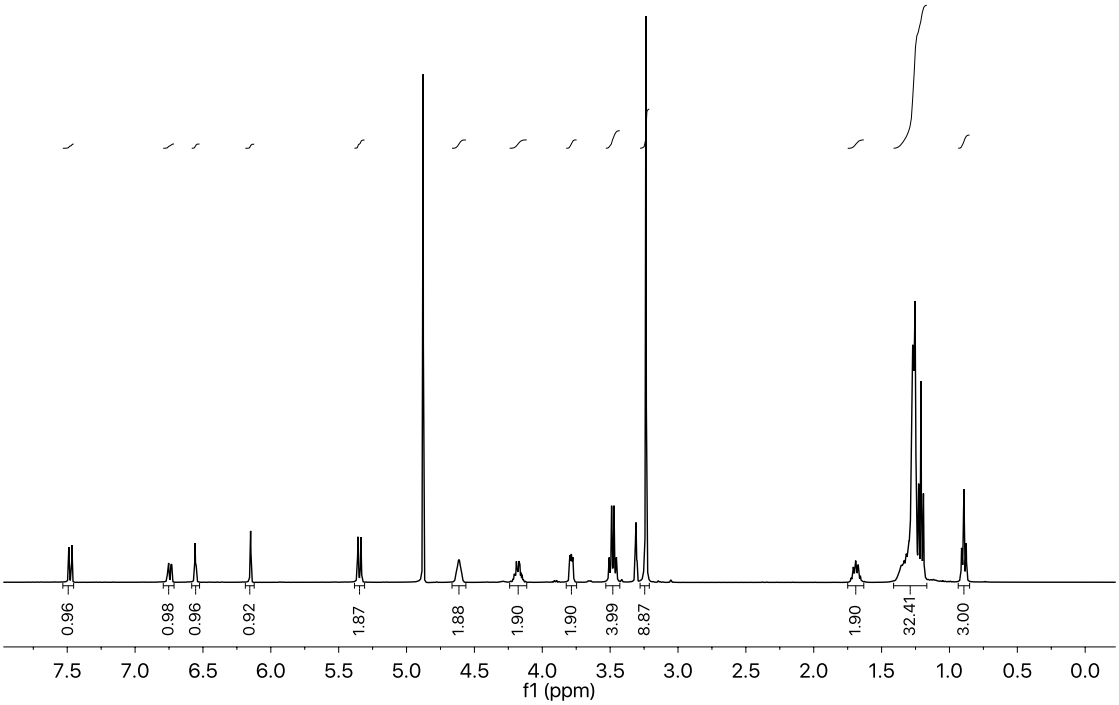

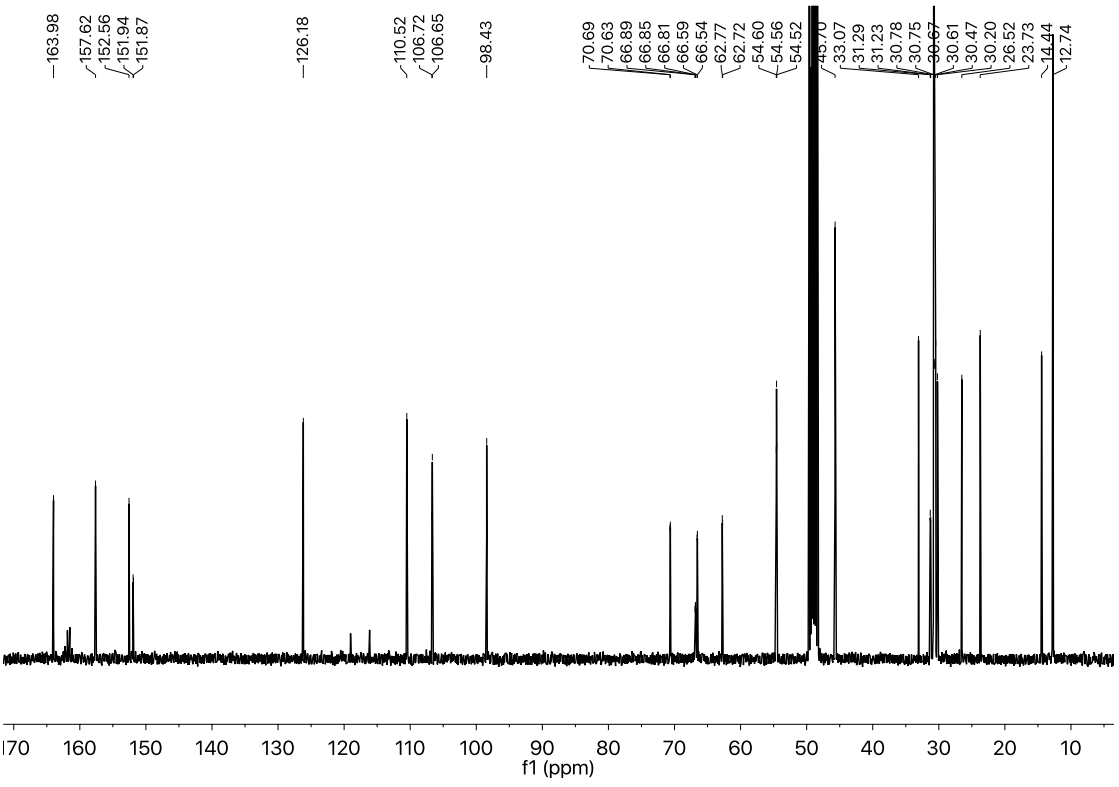

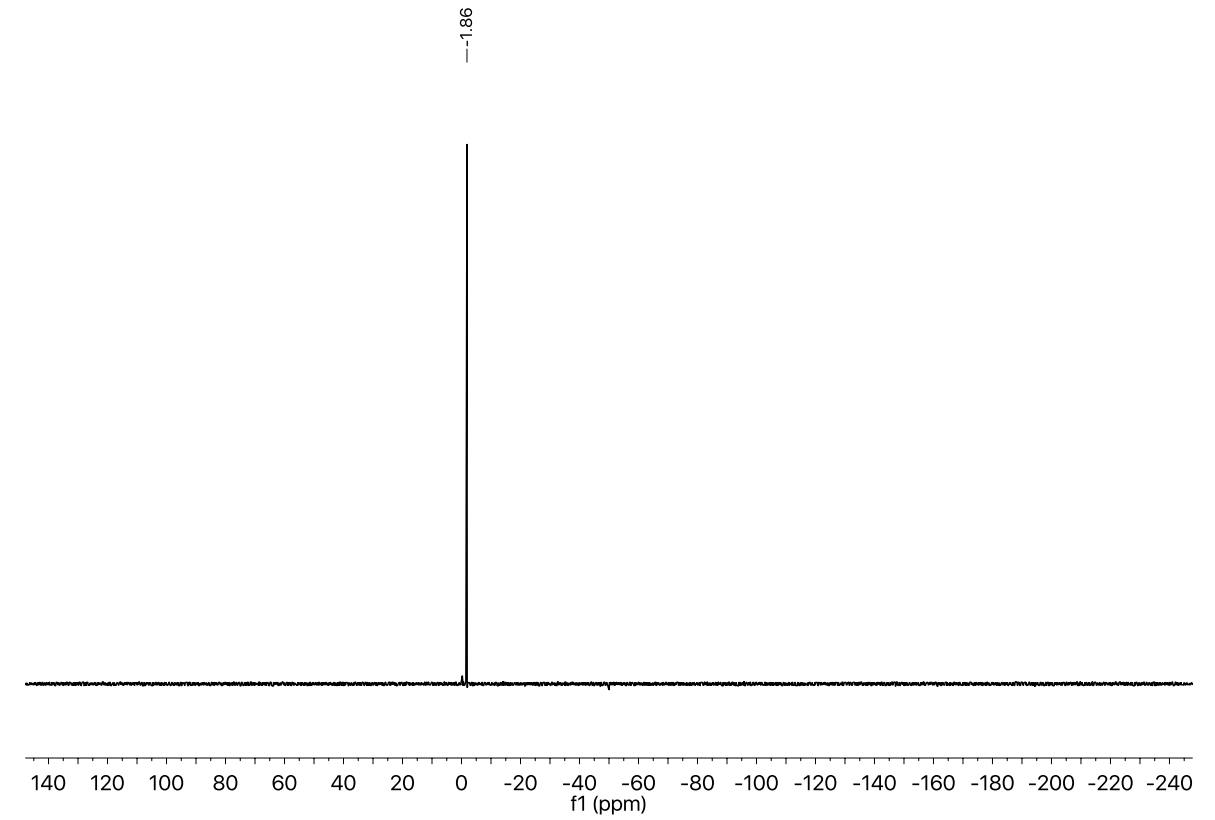
-1.86
140 120 100 80 60 40 20 0 -20 -40 -60 -80 -100 -120 -140 -160 -180 -200 -220 -240
f1 (ppm)

(**12**, cg edelfosin)

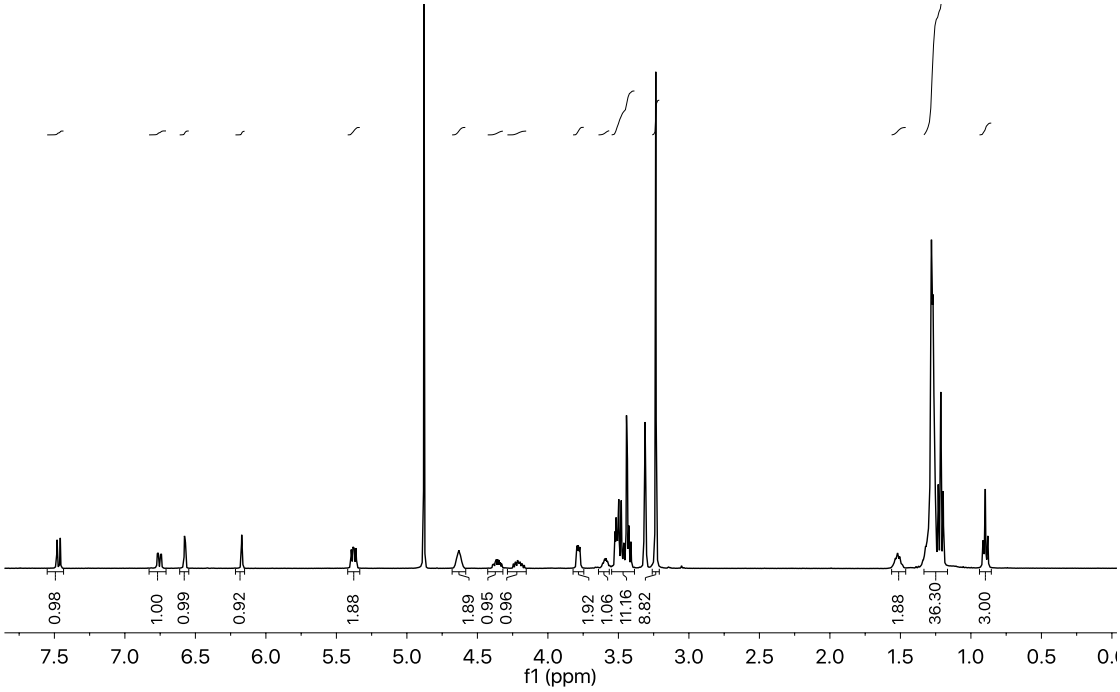

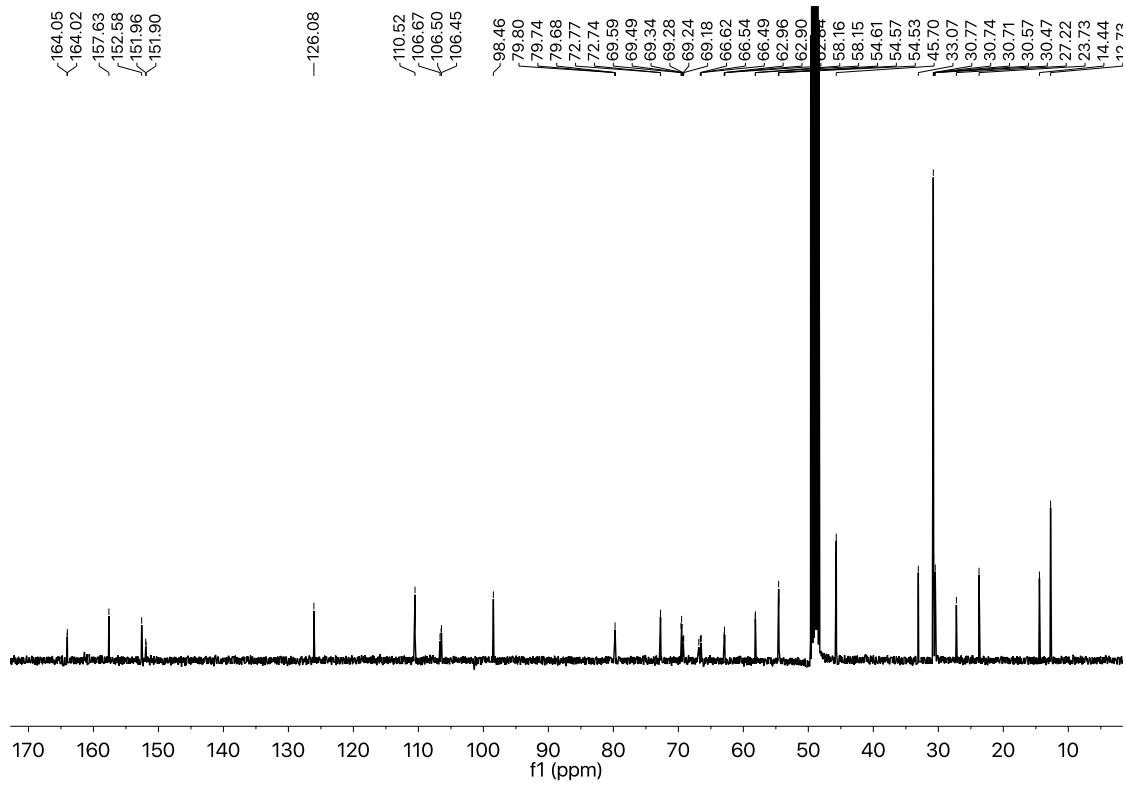

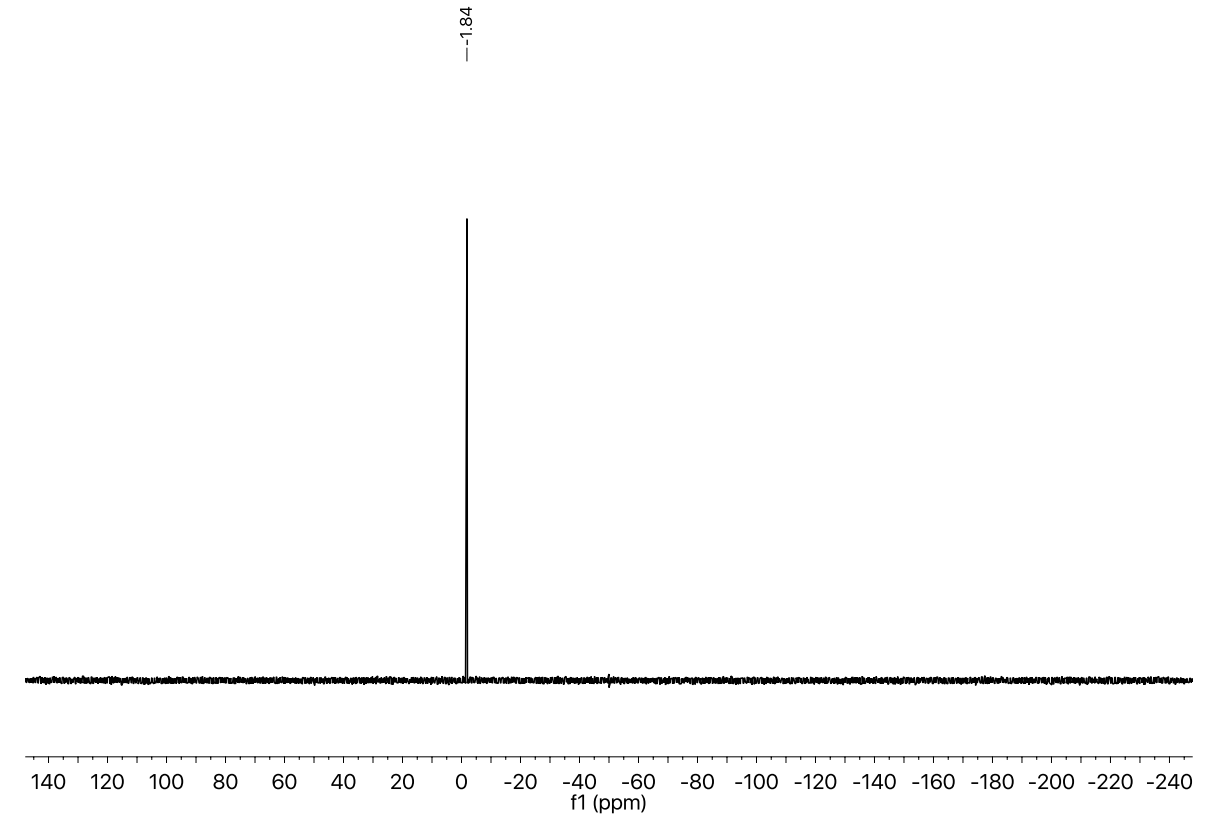
-1.84
140 120 100 80 60 40 20 0 -20 -40 -60 -80 -100 -120 -140 -160 -180 -200 -220 -240
f1 (ppm)

(**13**, cg PGE_2)

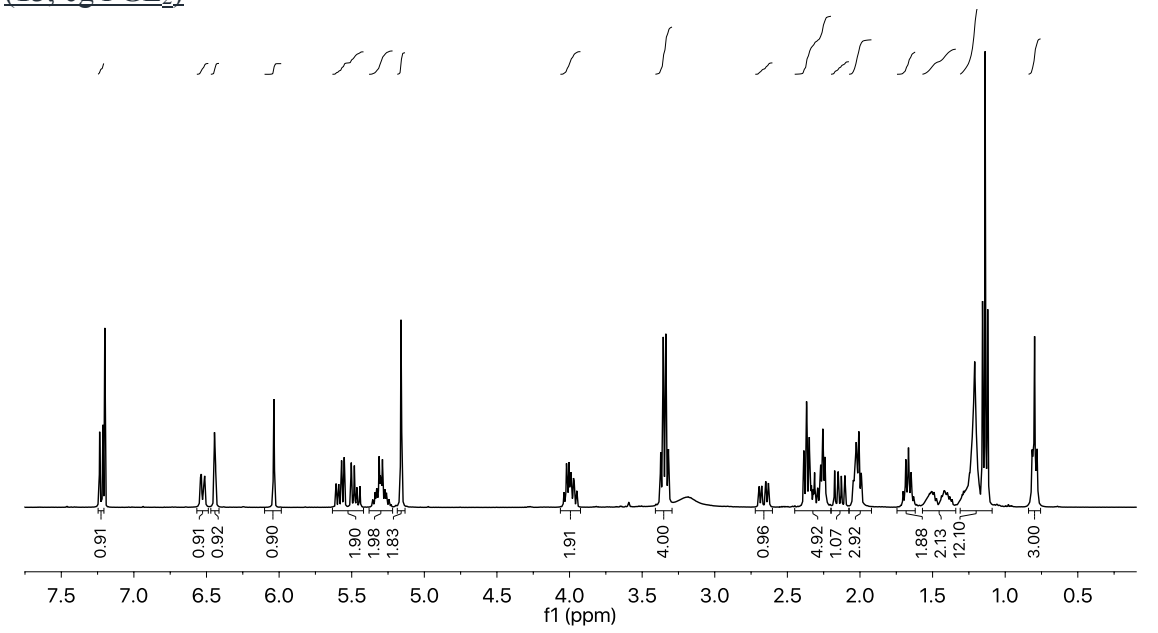
0.91
0.91
0.92
0.90
1.90
1.98
1.83
1.91
4.00
0.96
4.92
1.07
2.92
1.88
2.13
12.10
3.00
7.5 7.0 6.5 6.0 5.5 5.0 4.5 4.0 3.5 3.0 2.5 2.0 1.5 1.0 0.5
f1 (ppm)

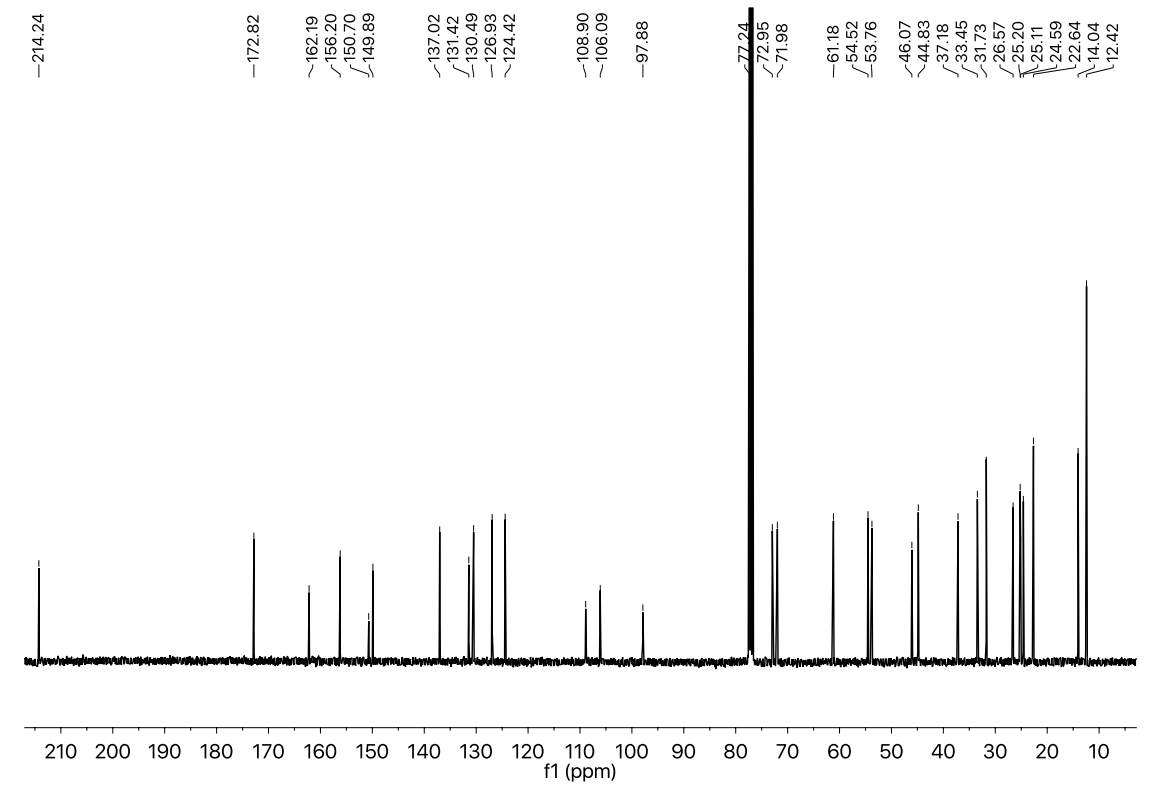
214.24
172.82
162.19
156.20
150.70
149.89
137.02
131.42
130.49
126.93
124.42
108.90
106.09
97.88
77.24
72.95
71.98
61.18
54.52
53.76
46.07
44.83
37.18
33.45
31.73
26.57
25.20
25.11
24.59
22.64
14.04
12.42
210 200 190 180 170 160 150 140 130 120 110 100 90 80 70 60 50 40 30 20 10
f1 (ppm)

(**14**, cg OHOA)

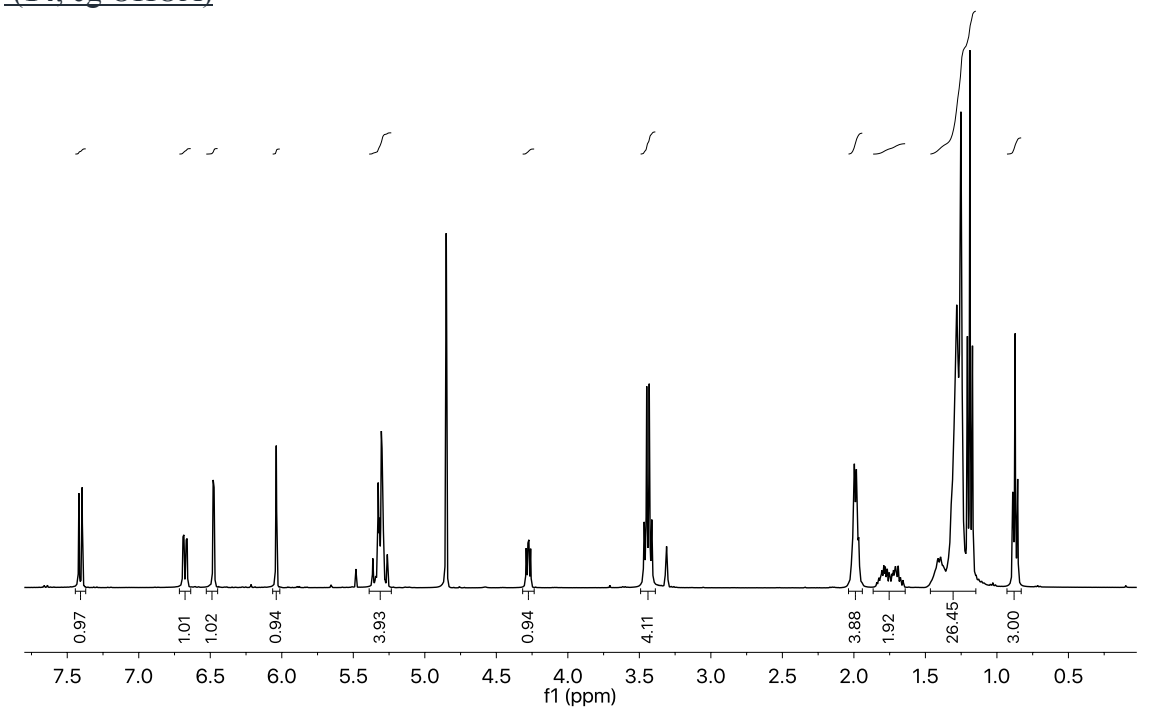
0.97
1.01
1.02
0.94
3.93
0.94
4.11
3.88
1.92
26.45
3.00
7.5 7.0 6.5 6.0 5.5 5.0 4.5 4.0 3.5 3.0 2.5 2.0 1.5 1.0 0.5
f1 (ppm)

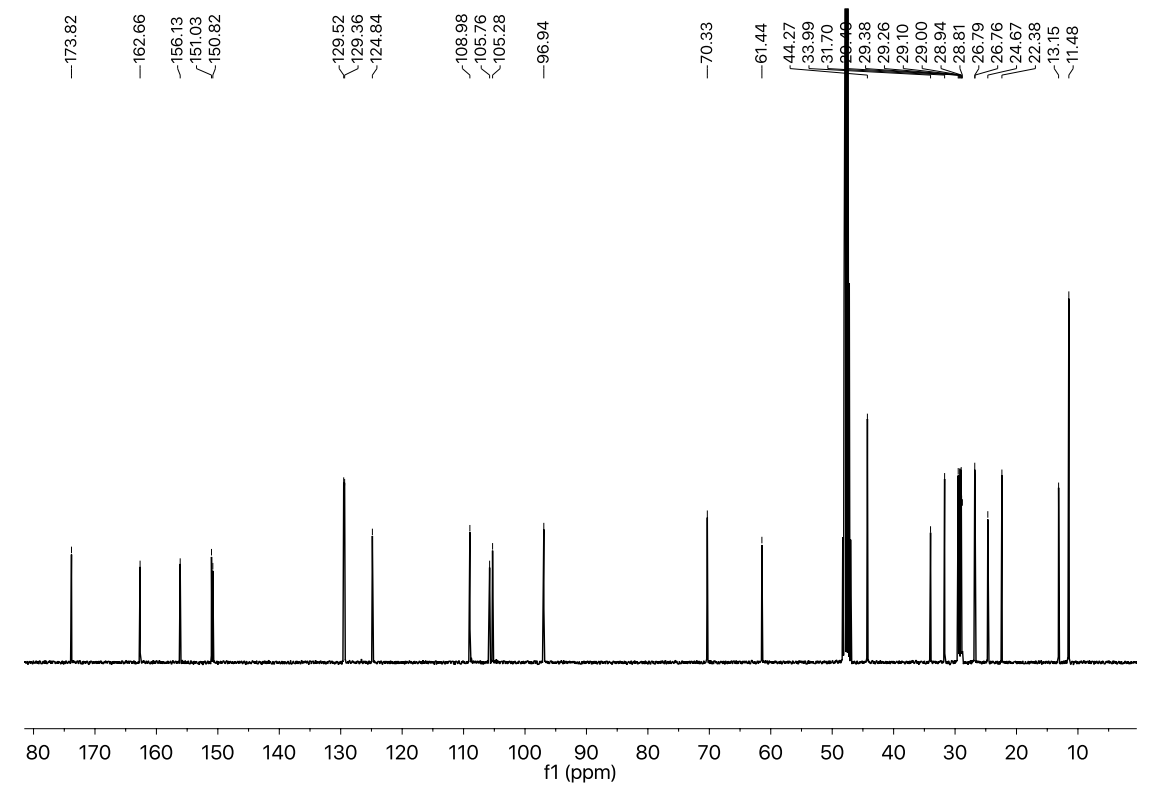
173.82
162.66
156.13
151.03
150.82
129.52
129.36
124.84
108.98
105.76
105.28
96.94
70.33
61.44
44.27
33.99
31.70
29.38
29.26
29.10
29.00
28.94
28.81
26.79
26.76
24.67
22.38
13.15
11.48
80 170 160 150 140 130 120 110 100 90 80 70 60 50 40 30 20 10
f1 (ppm)

(15, cg NANA)

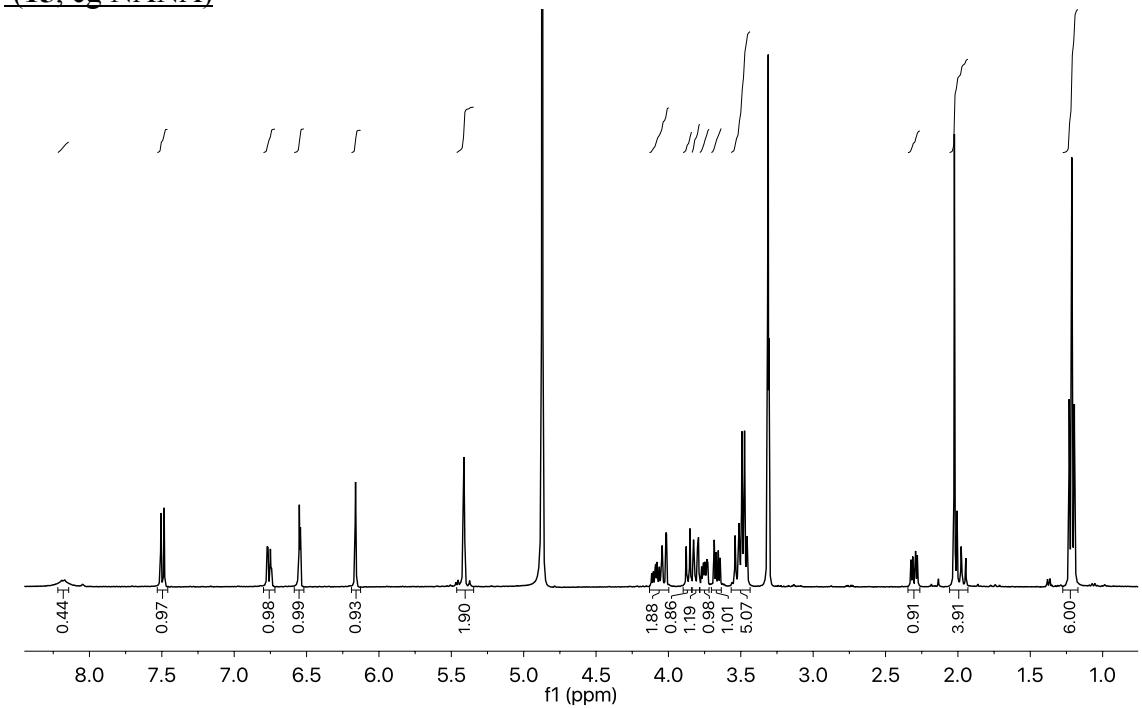
0.44
0.97
0.98
0.99
0.93
1.90
1.88
0.86
1.19
0.98
1.01
5.07
0.91
3.91
6.00
8.0
7.5
7.0
6.5
6.0
5.5
5.0
4.5
4.0
3.5
3.0
2.5
2.0
1.5
1.0
f1 (ppm)

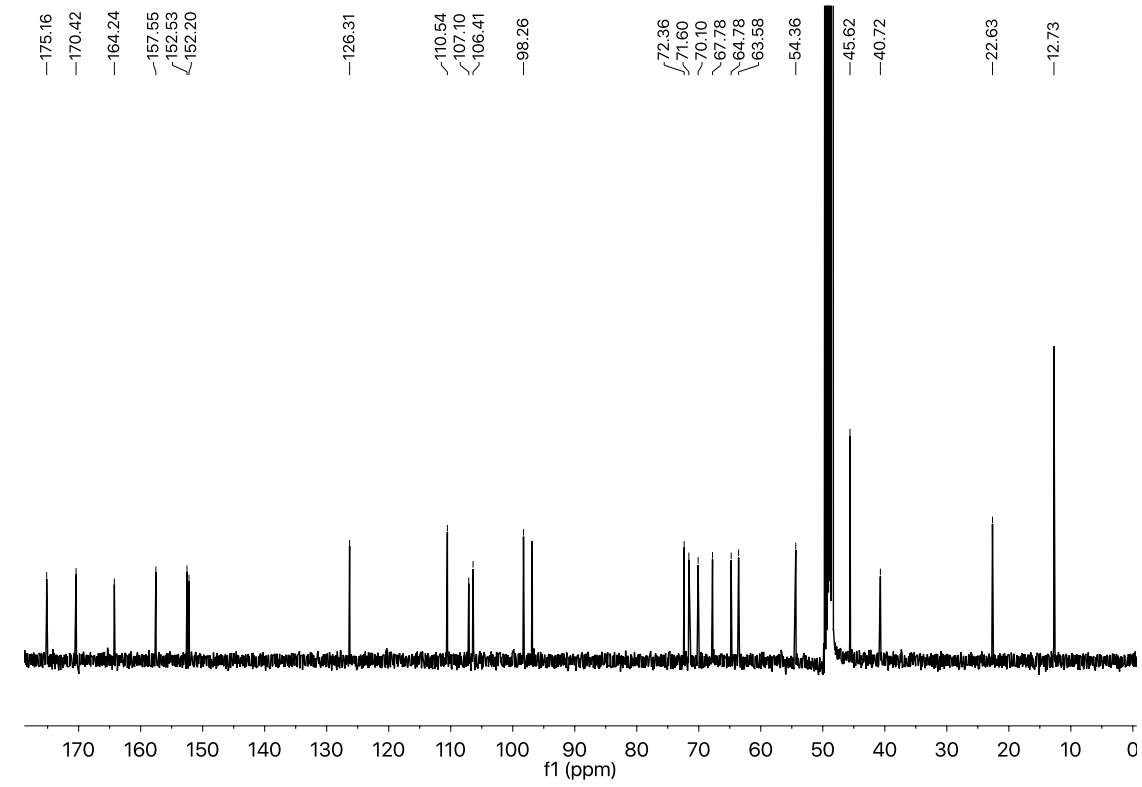
175.16
170.42
164.24
157.55
152.53
152.20
126.31
110.54
107.10
106.41
98.26
72.36
71.60
70.10
67.78
64.78
63.58
54.36
45.62
40.72
22.63
12.73
170
160
150
140
130
120
110
100
90
80
70
60
50
40
30
20
10
0
f1 (ppm)